CHALMERS

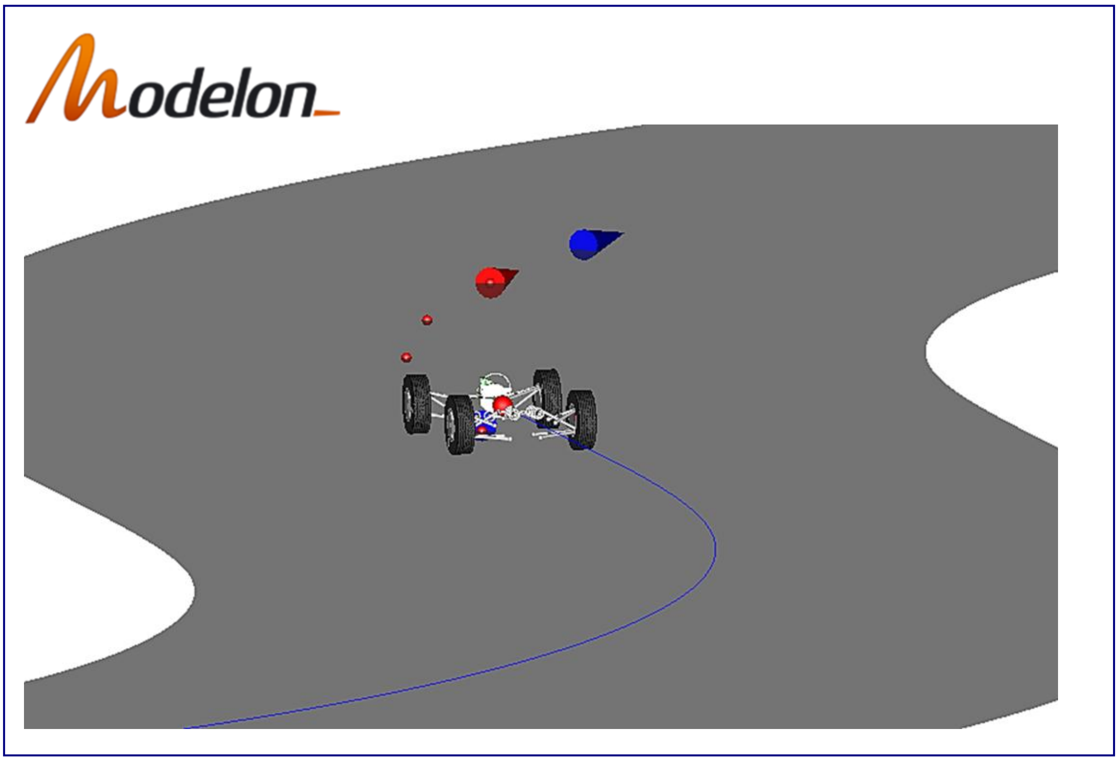

Development of Velocity planner for a Racing driver model

Part of Modelon AB's Vehicle Dynamics Library (VDL) for Dymola Multi-Physics software

Master's Thesis in the Master's programme in automotive engineering

ARUN KUMAR SUBBANNA

Department of Applied Mechanics
Division of Vehicle Engineering & Autonomous Systems
CHALMERS UNIVERSITY OF TECHNOLOGY
Göteborg, Sweden 2012
Master's thesis 2012:29

MASTER’S THESIS IN AUTOMOTIVE ENGINERING

Development of Velocity planner for a Racing driver model

Part of Modelon AB’s Vehicle Dynamics Library (VDL) for Dymola Multi-Physics software

ARUN KUMAR SUBBANNA

Department of Applied Mechanics
Division of Vehicle Engineering & Autonomous Systems
CHALMERS UNIVERSITY OF TECHNOLOGY

Göteborg, Sweden 2012

Development of Velocity planner for a Racing driver model
ARUN KUMAR SUBBANNA

Master's Thesis 2012:29
ISSN 1652-8557
Department of Applied Mechanics
Division of Vehicle Engineering & Autonomous Systems
Vehicle dynamics group
Chalmers University of Technology
SE-412 96 Göteborg
Sweden
Telephone: + 46 (0)31-772 1000

Department of Applied Mechanics
Göteborg, Sweden 2012

Development of Velocity planner for a Racing driver model
Part of Modelon AB's Vehicle Dynamics Library (VDL) for Dymola Multi-Physics
Master's Thesis in the *Master's programme*
ARUN KUMAR SUBBANNA
Department of Applied Mechanics
Division of Vehicle Engineering & Autonomous Systems
Vehicle dynamics group
Chalmers University of Technology

ABSTRACT

Testing a vehicle's limit handling capabilities can provide a valuable insight into analysing and hence developing new vehicle designs. A driver model is a convenient tool used particularly in full vehicle simulations and if it is capable of simulating driving on the limit with minimum user input then it becomes all the more effective. There is inadequate information found in literature concerning the simulation of limit handling capability of a vehicle using a driver model.

There was a requirement to improve an existing driver model in Modelon AB's Vehicle dynamics library (VDL), so that it would enable the user find the limits of handling of a vehicle. This also had to be accomplished with minimum user input and without a priori information of the entire track. Furthermore, the vehicle model should be driven on the pre-defined path on the road accurately. Hence the speed calculation has to be accurate, capable of triggering braking, whenever required to successfully maintain the trajectory of the vehicle on the given path.

The targets of lateral and longitudinal acceleration/deceleration of the vehicle model were the only input specified by the user. The complete driver model was then to be used in closed loop driving manoeuvre simulations on a 2-D road. The velocity planning block, developed in this thesis, calculates the vehicle speed based on user inputs. It also utilises a limited look-ahead preview of the track and ensures that the vehicle model is pushed to the boundaries of these specified targets while at the same time maintaining the pre-defined trajectory. The tests are conducted on three different tracks; A circular track with constant radius, J-turn and an extended chicane

Two strategies were employed to solve the problem. First, a single-point look-ahead preview, where information about one point of the upcoming road curvature is known, is incorporated into the driver model. Later, in order to make the solution more robust, a multi-point preview is implemented. The velocity profile calculated was found to push the car to the specified targets and the velocity tracking was performed to a satisfactory level. The vehicle model accurately followed the pre-defined vehicle trajectory without a priori information of the track, and in the case of single-point preview strategy, the look-ahead distance required almost no fine tuning of the preview distance for the three tracks the model was tested on.

Key words:

Driver model, velocity planning, limit handling, full vehicle simulation

Contents

Preface

In this thesis dissertation, improvements were made to a driver model such that it could effectively simulate limit handling driving manoeuvres. This was carried out from September 2011 to February 2012. The project conducted at the premises of Modelon AB in collaboration with the Division of Vehicle engineering and Autonomous systems, Department of Applied Mechanics, Chalmers University of Technology, Sweden. Part of this thesis will also be published in the proceedings of the 11th International Symposium on Advanced Vehicle control in association with the Japan Society of Mechanical Engineers (JSAE) [10].

The project has been carried out with Ph.D. Fredrik Bruzelius as examiner from Chalmers and Ivar Torstensson as advisor at Modelon AB. This was executed in coordination with Umair Ahmed, Master's student in control engineering from Karlstad University. All simulations have been using Dymola software. The driver model is intended to be a part of Modelon's Vehicle dynamics library. Department head of Vehicle dynamics at Modelon, Eng. Edo Drenth are highly appreciated for their help with his guidance and Peter Sundstöm for proposing the idea for the thesis.

Göteborg March 2012

Arun Kumar Subbanna

Notations

t	Time
s	Distance
ds	Small increment in distance
v	Vehicle speed
v_{max}	Maximum vehicle speed
v_i	Velocity at any point i on the track
v_x	Predicted Longitudinal velocity
$\dot{v}_x$	Predicted Longitudinal acceleration
a_y	Lateral acceleration
$a_{y,max}$	Maximum lateral acceleration, specified by the user
$a_{y,i}$	Longitudinal acceleration at any point i on the track
a_x	Longitudinal acceleration
$a_{x,max}$	Maximum longitudinal acceleration
$a_{x,i}$	Longitudinal acceleration at any point i on the track
m	Vehicle mass
r	Path radius
k	Path curvature
k_{max}	Maximum Path curvature
μ	Friction
g	Acceleration due to gravity
$\Delta\theta$	Increment in distance
F_y	Lateral force
F_z	Normal load
δ	Steering wheel angle
β	Vehicle side-slip angle
$tanh$	Tangent hyperbolic function
K	Tuneable slope of the tangent hyperbolic function

1 Introduction

1.1 Background

A key tool in determining the handling characteristics of the vehicle is a lap simulation environment. One of the most convenient ways to perform a lap simulation involves driving a mathematical full-vehicle model on a pre-defined track, using a driver model. During the course of the lap, all the necessary measurements can be taken and thus the performance envelope of the vehicle determined.

If the driver model was capable of pushing the vehicle to edge of its performance limit at every section of the track, then this would provide an effective technique to determine the limit handling capabilities of the vehicle. To perform an effective lap simulation, the user has to define a “Velocity profile”. A velocity profile is nothing but the velocity defined as a function of distance along the track. This pre-defined velocity has to be defined at every point on the track. Defining this is quite a cumbersome job for a user. Also taking into account the exact track layout when calculating the velocity profile is no easy task*, See* 2.1.1

This dissertation focuses on calculating a “Velocity profile” with **minimum user input** and **with limited a priori information of the track layout.** The objective of the velocity planning strategy developed in this thesis is to calculate a velocity online, given the road environment, such that the vehicle is driving on the handling limit without losing control or path. Two “velocity planning” strategies which constitutes a part of the driver model is presented here. These strategies was implemented in the Vehicle dynamics library (VDL) developed by Modelon AB for Dymola multi-physics software (Dassault Systèmes) [6].

1.2 Driver Models in VDL:

The driver model performs the task of virtually driving a vehicle model along a pre-defined reference path on the road. This task is accomplished by controlling the different sub-systems which are responsible for navigation of the vehicle, such as steering wheel, accelerator and brake pedal and gear-shifting. The driver model acts on all these sub-systems simultaneously and in a co-ordinated fashion. These control actions are, of course, dictated by the interpretation of the driving environment, for example the curvature of the path at a specified distance (termed as ‘look-ahead’ distance) and the vehicle states such as speed, engine rpm etc. It is also evident from the above description that the driver model needs a complete vehicle with chassis, engine, braking and transmission systems and here in lies the difference with a robot [6].

Driver models are broadly classified into two categories, see e.g. [6]. They are:

Open-loop driver models:

This involves the control of only a signal that actuates the steering system, usually such that it follows certain pre-defined paths that simulate standardised manoeuvres such Lane-change, fish-hook, J-turn among others. The initial velocity is pre-defined and the manoeuvre is executed as an open loop system which means that if the vehicle strays from the pre-defined path then no corrective measures will be executed.

Closed loop driver models: These are the most commonly employed driver models in lap simulation. A pre-determined reference path can be defined on the ground, along which the vehicle is intended travel. Then velocities can be defined at different points along the path. The control actions executed by the driver model are intended to follow the defined path at the specified velocities. These actions are, by definition, executed in a closed loop, meaning that if the vehicle strays from the reference path and/or the reference velocity, corrective measures are taken.

In the VDL, the driver models are divided into three processing layers [7]:

Perception:

Perception is a block defined such that it contains the inputs from all internal sensors from the chassis as well as the driver controllers. It conveys the position of the vehicle along the path and its velocity, acceleration and other states that are necessary to perform calculation for tracking and planning.

Planning:

The planning block utilizes the information that it receives from the perception block. Based on the current position and vehicle velocity, it calculates driver frame coordinates from the preview points and the reference velocity as defined in a velocity profile.

Tracking:

The tracking block performs the control actions as specified by the planning block. The steering wheel angle is calculated based on the future position on the reference path as described by the planning block while the accelerator, brake, clutch and gear shift pedals are actuated to achieve the reference velocity at the future position as described by the planning block.

Block Diagram:

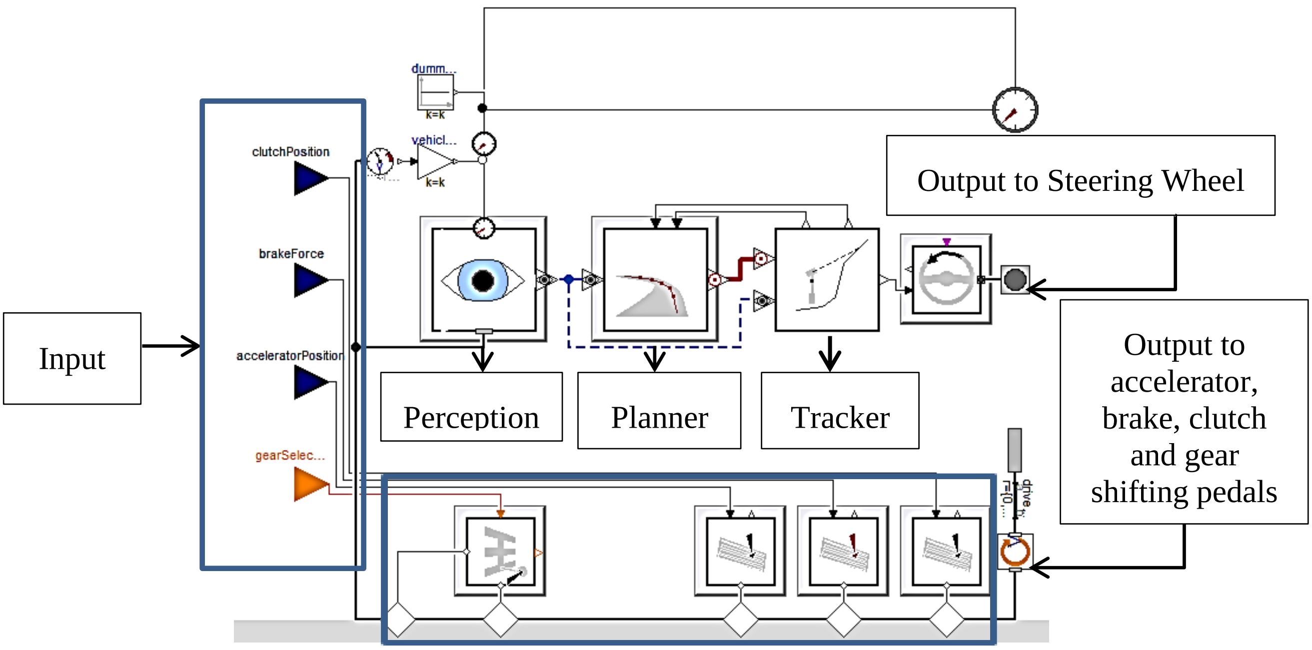

Figure 1: Block diagram of a closed loop driver model

1.3 Objective

The objective of the current master thesis is to improve the performance of the current driver model to an extent where it can be used to evaluate the limit handling performance of a vehicle.

The current driver model available within VDL has two disadvantages.

1) The velocity profile has to be manually specified by the user for a given track
2) The lateral tracker is a single point tracker, which results in corner cutting and off-tracking in tight corners at high vehicle speeds.

Therefore this project is broadly divided into two parts that include improving the velocity planning and the tracking controller. The first one is dealt with in this thesis.

1.3.1 Velocity planning:

Given a pre-defined path on the road, the vehicle should track this path as fast as possible, utilizing as much of the performance as it can extract from the tyres and the engine.

Based on parameters of the given vehicle, the velocity planning module should compute the maximum possible speed at any given point on the reference path. This is termed as a 'Velocity profile'. The longitudinal controller tries to tracks down this velocity profile.

The velocity profile that can be used in the feed-back or feed-forward loop of the existing PID controller that controls the actions of brake and throttle (from here on referred to as longitudinal controller) in Dymola

1.3.2 Steering Controller:

The steering controller executes closed loop control actions on the steering such that the deviation from the pre-defined path is kept to a minimum. This controller is independent from the velocity planning block.

This report will focus only on the calculation of the velocity profile executed by the **Velocity planning** module, from here on referred to as the **Velocity planner** and integration with the longitudinal controller and the subsequent results from simulations on different circuits. The steering controller was developed by co-worker Umair Ahmed. This work was published as a separate Master thesis in [9].

1.4 Delimitations

This master thesis focuses on deriving and implementing the velocity planner on simulations that are to be run on a 2D track, is considered to be completely flat with no banking, uphill or downhill sections.

As a rule of thumb, since it is for "Racing driver model", the minimum turn radius must not be too small when compared with the vehicle's wheel base. The centre-line of the road is assumed to be the "racing line" as the curvature for paths off-centre cannot reliably calculated at present. Also the curvature of the road-file is assumed to be smooth, without unreasonable abrupt changes.

The user may fine tune the preview distance if the need arises due to excessive complexity of the track.

The velocity planner has not been implemented for vehicles with aerodynamic downforce; hence if a car with an aero pack is used, it might be not reach limits of its handling.

2 Theory

2.1 Literature survey

Over the course of development of simulation tools specialized for the automotive industry, a number of driver models have been implemented. A literature survey was carried out in order to investigate different strategies and implement the one that best integrates with existing driver model in Vehicle dynamics library of Dymola [5].

This report treats the findings of the survey with respect to literature found on maximising the velocity travelled along a path to achieve limit handling.

There are two distinctive approaches to maximize the velocity travelled by a vehicle around a given track:

1) Off-line computation of the ideal racing line and the velocity profile
2) On-line dynamic computation of the velocity profile using vehicle states and information about the track.

2.1.1 Off-line computation methods:

The basic principle of this approach is to minimize the time consumed to go around a given track. There are several algorithms that can be implemented which treat the time taken to complete a lap as a cost function and apply the vehicle performance limits as boundary conditions. This eventually results in a definition of an optimised 'racing line', an optimum path for a given track along which the vehicle has the highest average velocity.

In [5], the problem is formulated as follows:

1) Minimize time taken around a track such that,

$$t = \int \frac{1}{v}\, ds \tag{2.1}$$

2) The maximum allowable velocity of a body of mass m around a curve of radius r is regulated by,

$$\frac{mv^2}{r} \leq \mu m g \tag{2.2}$$

3) If $\frac{1}{r} = k$, the curvature then,

$$kv^2 - \mu g \leq 0 \tag{2.3}$$

4) The car travels a distance of ds if it subtends an angle $\Delta\theta$ at the centre of the curve whose curvature is given by k

$$\int k ds = \Delta\theta \tag{2.4}$$

5) A minimum turning radius or maximum limit on the curvature specified below which the vehicle cannot turn into the curve.

$$k \leq k_{max} \tag{2.5}$$

6) The maximum limits on the velocity and acceleration capability of the vehicle is defined by engine performance

$$v \leq v_{max} \tag{2.6}$$

$$a_{min} \leq a \leq a_{max} \tag{2.7}$$

Where, a_{min} is defined as the deceleration limit, defined by combines capacity of brakes and tyres

He proposes 4 methods to accomplish this task.

- Euler spiral Method
- Non-Linear Programming Solver Method
- Artificial Intelligence method
- Integrating Euler and AI methods

Details of the above methods are not discussed here. However the primary condition to all race line optimization algorithms mentioned in this text is that the knowledge of the track be known beforehand, i.e., information about the ground curvature and length of the track. The AI code uses a brute force approach where a number of points along the road width are sampled and then the shortest time to travel around the track is calculated. The longer the track the more complex and computationally heavy it gets, requiring a minimum of 30000 iterations.

In [6], another offline algorithm that are implemented using a Modellica code. The concept of optimal linear preview as described in [4] has been implemented. The vehicle models implemented are simplified. The standout feature is that the track is broken down into smaller segments, after which a local optimum is calculated and then assembled, after which a global optimum is calculated. It would be interested to implement these algorithms and then incorporate the resulting velocity profile and 'racing line'.

The most comprehensive off line lap simulation technique is described in [3]. This is the Lap Time Simulation (LTS) program which makes use of techniques like the Milliken Moment method (MMM) and the G-G diagram, both of which are described in detail in section 2.4.

Dynamic Characterisation

Another school of thought of course is to implement the velocity planning online, as feed-forward or feed-back signals to a PID controller. This ensures take into account the dynamics involved in the driver model and the vehicle states to predict the future velocity.

A dynamic characterization of a vehicle is executed in [2], after which a racing driver model is developed. This involves performing a number of open-loop manoeuvres on the vehicle to determine not only the limits on longitudinal acceleration, but also on lateral acceleration. A look-up table which consists of longitudinal acceleration vs. velocity and lateral acceleration vs. velocity is constructed. Based on these limits the lateral planning to define the ideal "racing line" is calculated.

A speed profile is calculated and limits, resulting from the dynamic characterisation are applied as follows:

$$\frac{v_{i\ max}^2}{r_i} = a_{y,max}(v) \tag{2.8}$$

Where, v_i is the velocity and r_i is the radius at the i^{th} point on the track and $a_{y,max}(v)$ is the maximum acceleration which is now a function of the velocity after the dynamic characterisation.

The velocity calculated is limited by the following constraints on longitudinal acceleration and deceleration:

$$a_{x,i} = \min\left[a_x(v_i), a_{x,max}\sqrt{(1 - \left(\frac{a_{y,i}}{a_{y,max}}\right))}\right] \text{ - Acceleration} \tag{2.9}$$

$$a_{x,i} = \max\left[a_x(v_i), a_{x,max}\sqrt{(1 - \left(\frac{a_{y,i}}{a_{y,max}}\right))}\right] \text{ - Braking} \tag{2.10}$$

Although this strategy ensures taking in to account the dynamics of the vehicle when calculating the racing line, the whole procedure is rather time consuming. One must keep in mind that this might be the ideal solution on a finished vehicle. Since the need is to implement a driver model that can be used during the development stage of a vehicle, where the exact dynamics character of the vehicle cannot be determined accurately, this method is not very ideal.

2.1.2 On-line dynamic computation:

Equation (2.9) and (2.10) represent the edge of the 'friction ellipse' or more commonly known as the 'G-G' diagram [3] This represents the boundary of the available friction that can be utilized by the tyres, see section 2.4.

This strategy was implemented by [1]. A feed-forward controller implemented such that it provides the appropriate value of longitudinal acceleration and deceleration such that the edge of the friction circle is traced. Appropriate limits are applied on the signal as well. It is calculated as follows:

By using Newton's second law, the maximum acceleration that the vehicle could generate is equal to μg, where g is the acceleration due to gravity and μ is the available friction limit.

$$(\mu g)^2 = a_x^2 + a_y^2 \tag{2.11}$$

The feed-forward longitudinal acceleration a_x is calculated by assuming a value of a_y as follows:

$$a_y = \frac{v(s)^2}{r} \tag{2.12}$$

$$a_x = \sqrt{\left(\mu g - \left(\frac{v(s)^2}{r}\right)\right)} \tag{2.13}$$

The velocity profile is obtained by integrating this value of acceleration along the length of the path.

$$a_x = \frac{dv(s)}{dt} = \frac{dv(s)}{ds} * \frac{ds}{dt} = \frac{dv(s)}{ds} * v(s) \tag{2.14}$$

The above mentioned approach is demonstrated on a symmetric Clothoid. A Clothoid or an Euler Spiral is a curvature whose radius increases linearly with distance. The track is as shown below

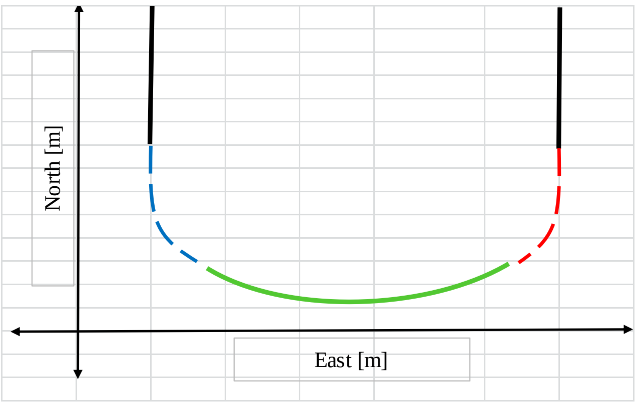

Figure 2: Clothoid track layout, Source - [1]

The two sections marked blue and red, are symmetric and equation (2.13) is first integrated backward, i.e., during an expanding curve (red section). The velocity in the Clothoid section marked blue, the equation is integrated backward. In the constant radius section, marked green, equation (2.12) holds good. Since the two curves are symmetric, there are no problems encountered. However, on a track with random curves this may not be feasible. The solution of equation (2.13) becomes complex if the curvature decreases abruptly. Hence it can be concluded that online calculation of the velocity profile between a_y may require manipulation between equation (2.12) and (2.13).

2.2 Defining limit handling

It is important to define what exactly “limit handling” means and what defines the edge of vehicle’s handling performance.

Consider a vehicle travelling around a curve of constant radius R, with a gradually increasing velocity. According to (2.8) the lateral acceleration a_y keeps increasing. Let us assume that the vehicle is in steady-state motion that is there is no net yaw-moment. For this condition to be satisfied, lateral acceleration has to be balanced by the lateral forces generated by both the front and rear axle slip, both of which increase with the increase in lateral acceleration.

Figure 3 shows normalized tyre forces v/s slip angle. Three distinct regions can be seen clearly. In the linear region the slip angle is proportional to lateral force. In the transitional region, the relationship between the two become non-linear while in the frictional zone, increase in the slip angle leads to no significant increase in lateral force, and sometimes even a decrease. At this point, the tyre/axle is said to be saturated.

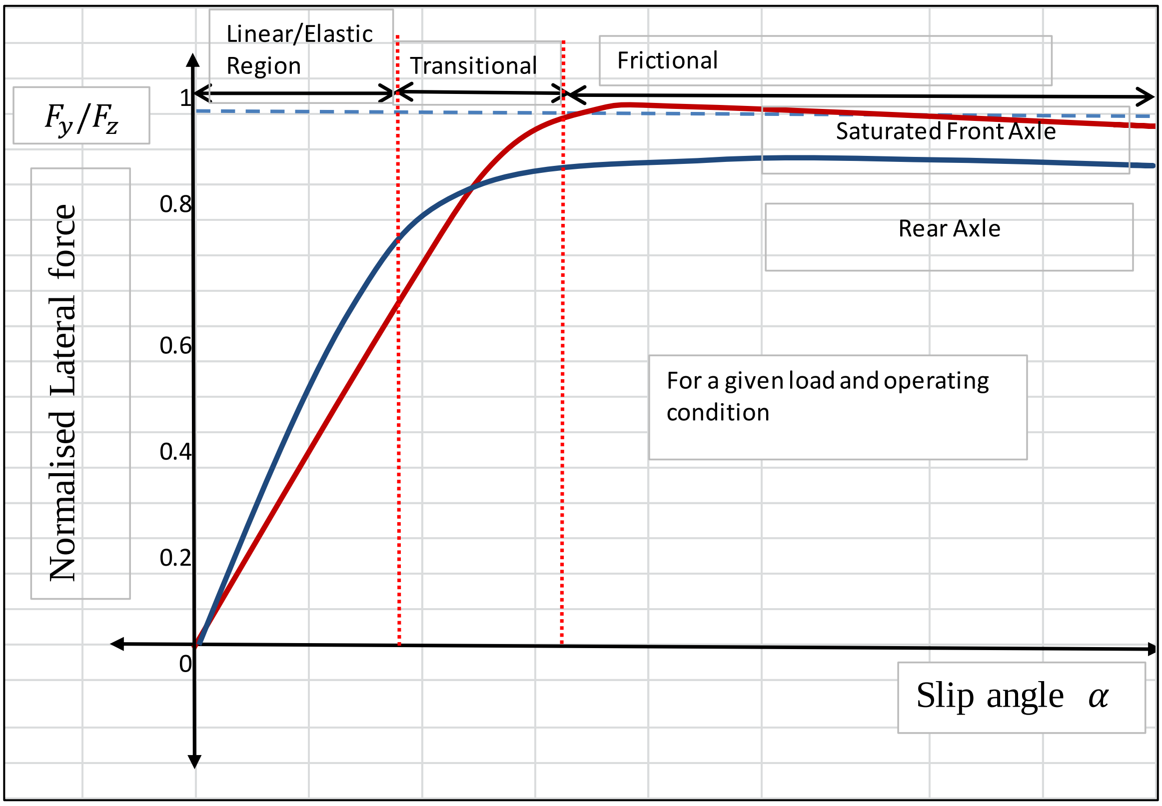

Figure 3: Normalized Lateral Force vs. Slip angle

To achieve the maximum possible velocity around a curve of given radius requires the vehicle to go around it with the highest possible level of lateral acceleration but at the same time with a yaw moment balance (steady-state condition). It is easy to see that this can only happen when the moment generated by the maximum lateral forces from the front axle balance that from the rear axle.

This can happen only when all four tyres peak or come close to their saturation values at the same time which means that they are utilizing all of their potential cornering force. The vehicle is said to be neutral and literally slides around, with minimal control. This can be defined as the very **edge of the vehicle's handling capability.**

It is impossible to achieve this "neutral" condition under all situations as various factors influences, see section 2.4. Figure 3 also shows that characteristics of the front and rear axles differ. This is one of frequently encountered situations due to the fact that these characteristics are governed by weight distribution, load transfer (during traction or braking) among others. When both the axles have reached the frictional or transitional stage then the vehicle is said to be in **limit handling mode**, see for example [3].

2.3 Limit performance

When both the axles are operating in their linear range, then the condition is referred to as on-centre handling. As can be seen from Figure 3, even in this region the differences in the cornering stiffness' between the front and rear axles cause understeer or oversteer, in this case, the situation being oversteer. This situation is usually encountered under 0.3 to 0.4 g for a non-aero car running on a dry high friction surface.

Above this value it is seen that the tires move into the transitional region. If the front axle's limit is reached first, as is the case in Figure 3, then for the same slip angle, there won't be any increase from the front axle. This means that for an increase in the steer angle in this condition will not produce the desired control action. The lateral force from the rear-axle which is still not saturated tends to straighten out the vehicle. This is termed as final understeer or in simple words the vehicle is said to "plough", [3]. In this condition the only possible mitigation manoeuvre is to reduce the speed or by braking the rear axles.

It must be noted that in this curve, the vehicle has lost the ability to turn more. In other words, if the vehicle is traveling on a closing curve and it reaches the condition illustrated in Figure 3, then it cannot be expected to turn in more without losing control. This condition is called "stable trim" [3].

When the limit is reached in the rear axle first, there is no increase in the lateral force from the rear axle and consequently no moment to balance the front axle. There is a risk that the moment due to the lateral forces from the front axle dominates and throws the vehicle into spin. There is no stability against small disturbances in this condition. This called the "unstable trim".

As mentioned earlier, the most ideal condition is when both front and the rear axles reach their saturations at the same time. In this condition the vehicle travels will drift, and will have not have the possibility of changing its trajectory until the axle slips reduce below their peak.

2.4 The G-G diagram:

"A method for characterizing the performance of the driver-vehicle system, including the influence of the roadway surface conditions … a means for quantifying the capability envelope of the car and demonstrating how much of this capability is utilized by the driver in the performance of the driving tasks"

- ***Roy S.Rice, Calspan corporation*** **[3]**

The concept of G-G diagram was first proposed by Roy Rice [3] who proposed that all the four tires can be related and combined into one diagram representing a car-road interface. The lateral force developed by a tyre is influenced by steering, braking/traction which in turn dictate slip angle and slip ratio [8]. But fundamentally this force is limited by the friction between the tyre and the road and how the tyre is loaded [3]. So basically for a constant load F_z

$$F_y = \mu F_z \tag{2.15}$$

Although it is an approximation, given the fact that it almost nearly impossible to track and measure the changes in the tread pattern at all times, this has proven to be effective [3]. Hence the name " Friction Circle/Ellipse" and if expressed in terms of lateral and longitudinal accelerations instead of force (as it is easy to measure) and plotted against each other, it is called the G-G diagram.

2.4.1 Limitations

Ideally all four tires should reach full utilization at the same time to achieve the maximum possible levels of acceleration. And if that were the case then the vehicle could easily reach the limit of the friction circle. The following reasons explain so as to why this is not possible:

1. **Power Restriction**:
   The upper limit for velocity is primarily restricted by the output from the vehicle's powertrain. Even if the friction is not a limitation (say for example on a straight line) all of it isn't utilized as the power is incapable of producing sufficient slip ratio for maximum resultant force.
2. **Longitudinal and lateral load transfer:**
   The term F_z in (2.15) refers to the normal load on the tyres. As the vehicle manoeuvres on the road, depending on the suspension geometry (anti-dive and anti-squat) and parameters like roll stiffness, wheel rate [8], [3] etc., the normal load varies. Here is where tyre load sensitivity comes into picture. The load transfer will make it very hard to have the same utilization on all four tires as the absolute force levels that can be exerted are dependent on the normal load
   Influence of the Suspension:
   In addition to the suspension geometry, entities like Camber, Toe and compliances in the suspension geometry due to rubber bushings and mechanical deflections can alter the tyre contact patch with road under different circumstances such as roll, bump and other steering events. This directly influences the tyre forces.
3. **Limit handling behaviour:**
   As discussed in section 2.3, condition of every tyre during limit cornering varies. This results in understeer/oversteer/drifting which in effect prevent the full utilization of the friction circle.
4. **Brake Balance:**
   This parameter may prevent the simultaneous utilization of the friction by both the vehicle's axles.

2.4.2 Use of the "G-G" diagram in Lap-Time Simulation (LTS)

The advantage of the "g-g" diagram is that it purely focuses on handling performance and it moves away from the limitations of vehicle's stability and control. Apart from the fact that it helps to establish a boundary for vehicle's performance in an understandable manner, it also serves the purposed of evaluating the driver capability, in this case, the driver model. It is seen that the fastest drivers have a very smooth driving technique. When the G-G diagram is plotted after their drive, it is seen that they are operate on of the edges of the G-G diagram most of the time, thus minimizing lap time, [3]. Hence this technique was adapted by Milliken Research Associates to implement a lap-time simulation (LTS) environment. The primary goal is to find out the "theoretical" handling limit that will be achieved when “perfect driver” drives the vehicle. In order to find this out, MMM technique is used and is described below:

Milliken Moment Method (MMM):

A mathematical vehicle dynamics model is analysed for various combinations of steer angles and vehicle side-slip angles for a range of lateral accelerations. For a certain combination of steer angle and vehicle side-slip, the maximum steady-state lateral acceleration is achieved when the yaw-moment at the centre of gravity (CoG) resulting from the lateral forces at the tyres, is nearly zero. It must be noted that this state is temporary and lasts as long as the velocity is held constant. The plot of yaw moment v/s lateral acceleration is called Milliken moment method (MMM) diagram *See* Figure 4.

With the help of MMM, the friction circles at all four wheels and ultimately the friction circle for all four wheels can be calculated as follows:

- The lateral force vector for each vehicle is calculated and a friction circle is drawn, the radius of each being calculated according μF_z
- Vector addition of the forces at each wheel is done to find the resultant force vector which corresponds to that particular operating condition
- The sum of radii of all friction circles at each tyre gives the radius of the final friction circle. *See* Figure 5

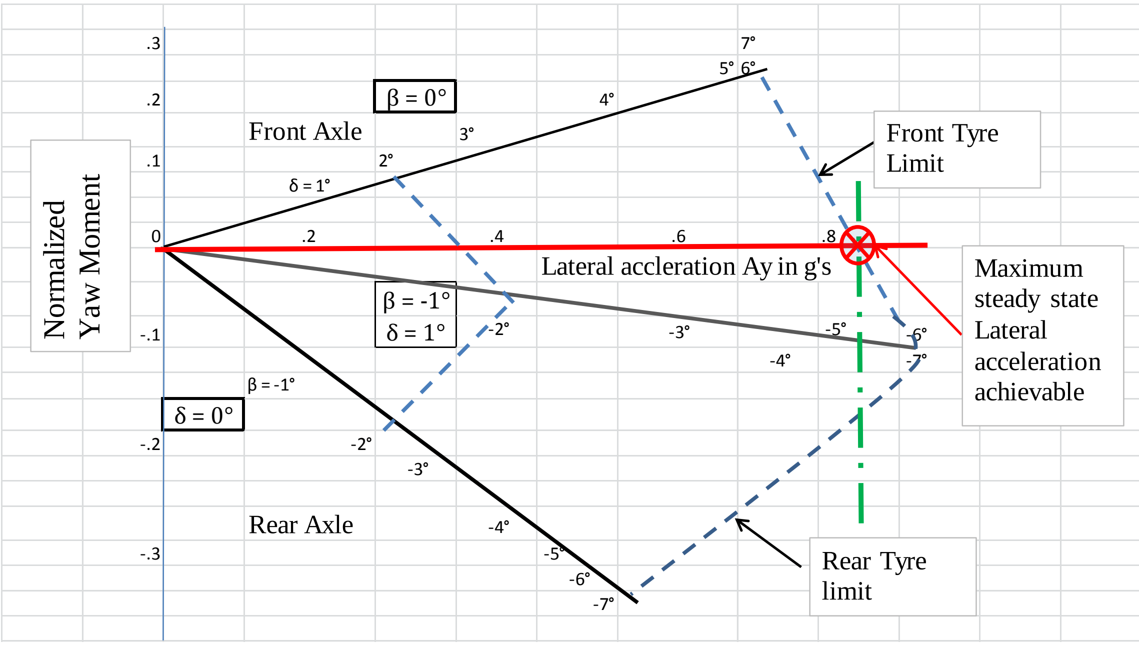

Figure 4: MMM Diagram indicating the max lateral acceleration achievable; Source-[3]

Left

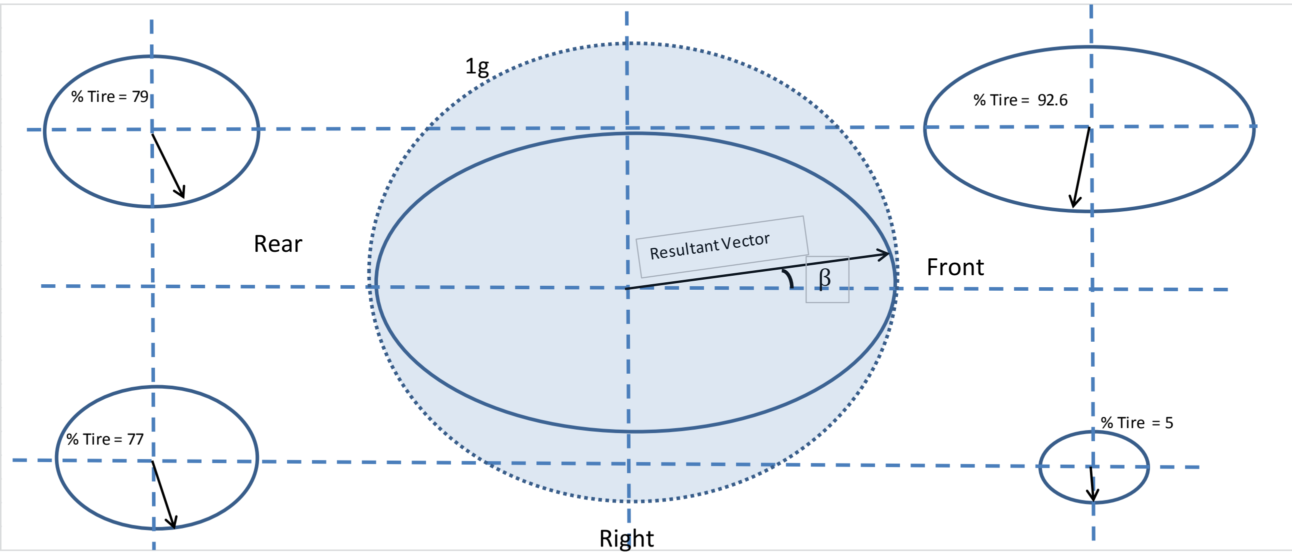

Figure 5: G-G diagram: Conditions indicated for all 4 wheels

Vehicle speed = 100 mph, δ =53.95°, β = -4.434°; Source: [3]

Figure 5 represents the handling limit for one combination of steer angle, vehicle side slip and velocity, assuming a steady state condition. Hence the challenge in determining the “G-G” boundary that would be valid in several if not all conditions is not hard to imagine. The LTS program constructs numerous individual MMM, at different levels of drive torque and brake line pressure. The final G-G diagram used in the simulation is composed of points and every point is basically a snapshot of a momentary steady-state cornering at particular velocity with constant speed or braking. It uses a non-linear vehicle model where tire data and vehicle parameters are input. The race track is discretized into smaller sections of random length (around 3 to 5 metres) and steady-state trimmed solutions using MMM diagrams are computed. Using this data, the final G-G diagram of the vehicle is constructed.

One of the most important aspects of a G-G diagram is that its shape becomes a function of vehicle speed in the case of vehicles with an aerodynamics package that creates downforce. The amount of downforce increases with the square velocity, and hence the envelope of lateral acceleration keeps increasing with it. The LTS program uses velocity dependant G-G diagrams.

Due to the sheer complexity of this whole setup and the need for online causal time computation, the present work purely utilizes a very simplified equation representing the friction ellipse as a reference for calculating the ideal speed with which the vehicle should be driven, the details of which are found in the next chapter. This was done mainly to keep the parameters that the user needs to a bare minimum and thus increasing the robustness of the model.

3 Methodology

3.1 Research Method:

The strategy implemented in this paper makes use of the concept of linear preview; a concept successfully utilized in, for example, [4] to implement a steering controller for a driver model. This involves obtaining information about the upcoming road environment by looking-ahead of the vehicle. The magnitude of this distance should ideally follow the law of optimal linear preview, which states that the controller does not utilize the preview information beyond a certain a limit.

This look-ahead or preview distance is utilized to find the information about the upcoming road curvature. Then subsequently the maximum velocity at this distance is found and then acceleration and deceleration limits are applied based on the user input. The user inputs are the desired approximations of longitudinal and lateral acceleration capability, which form the boundary for a given vehicle's performance.

This process is executed in continuous time, as the vehicle is driven around a given track, thus generating a velocity profile instantaneously. The velocity profile calculation involves computing the present vehicle states, user input and preview information in a manner which would ensure that vehicle is close to the edge of friction ellipse.

Also a point worth mentioning again is that the centreline of the track is assumed to be the racing line and the velocity profile is computed based on the curvature information of this centreline path. This was due to the difficulty of calculating online, the curvatures for paths that deviate from the centreline of the track. The optimal path or the racing line determines the time taken around a lap, and has a significant impact [5]. It is important to stress the fact that the focus here is on exploring limit handling capability of the vehicle and not to measure how quickly the vehicle travels round a track.

The velocity profile generated forms the input signal to a controller that operates on the throttle, brake and gear shifting mechanism. This is called the longitudinal controller and is in command of the longitudinal propulsion of the vehicle. This controller, which already exists in the present VDL implementation, tracks the input signal, the reference velocity profile. If longitudinal controller tracks its input successfully, then this would have pushed the vehicle to the limits of its performance.

3.2 Strategy implementation

One objective of the approach to solve the above mentioned problem is that the solution should be robust and be able to handle a variety of different vehicles. Hence, a simplified framework is used and the models involved in the computations assume that the vehicle can be expressed as a particle. For a particle, as well as for a quasi-stationary vehicle [3], the lateral acceleration a_y is given by (2.8) .

Where v_x is the longitudinal velocity and R is the curve radius of the path the particle is following. This equation represents the maximum possible velocity that can be achieved for a given value of lateral acceleration. Hence, this equation can be used to determine an upper limit of the vehicles longitudinal speed given simply re-writing (2.13)

$$\frac{v_{max}^2}{r} = a_{y,max} \tag{3.1}$$

The friction ellipse equation is used to combine the effect of lateral and longitudinal accelerations [2]. It determines the limiting acceleration envelope of the vehicle.

$$\left(\frac{a_x}{a_{x,max}}\right)^2 + \left(\frac{a_y}{a_{y,max}}\right)^2 \leq 1 \tag{3.2}$$

Here, $a_{x,max}$ and $a_{y,max}$ are the maximum possible accelerations that can be achieved in the longitudinal and lateral directions respectively. The maximum acceleration may be viewed as user inputs and can be determined by simple experiments. The inequality (3.2) is depicted in Figure 6, where the red ellipse indicates equality. It is reasonable to assume that if the velocity is equal to the limit velocity determined by (2.8) using the maximum possible lateral acceleration, an optimal strategy is achieved with respect to "lap" time or minimal time problems, where the path curvatures are optimised to achieve the above mentioned objective [5]. For straight lines the solution is trivial i.e. maximum acceleration, but may be implemented as an acceleration that relates to the acceleration capabilities of the vehicle. To reach the optimal longitudinal velocity in the general case assuming straights are curves with infinite curve radius; the vehicle needs to respect the friction limits given by (3.2). Combining (3.2) and (3.1) we get.

$$\dot{v}_x = a_x = \pm a_{x,max}\sqrt{1 - \left(\frac{v_x^2}{Ra_{y,max}}\right)^2} \tag{3.3}$$

A strategy can be obtained, where the sign determines if the velocity needs to be reduced or increased to reach the set point speed for any point on the track calculated using (2.8).

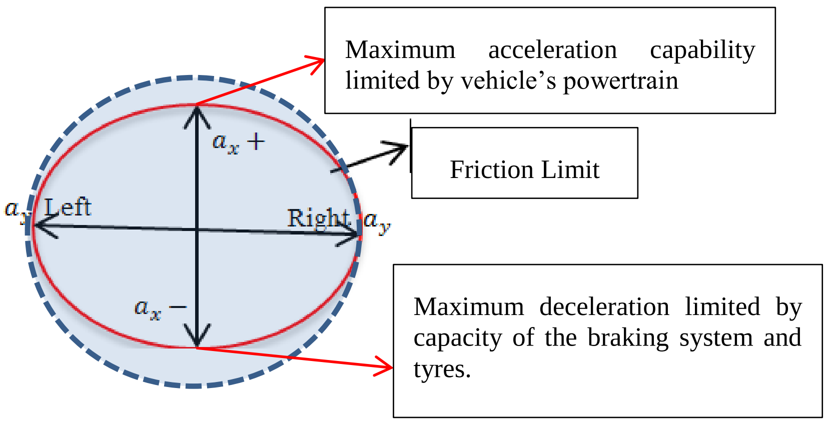

Figure 6: Friction Circle/Ellipse

It is not hard to see that the solution to (3.3) only exists for monotonically increasing curve radii, i.e. with reducing curvature. The velocity profile generated by (3.3) will not respect the friction ellipse for closing curves and reduce the velocity in advance as required to remain on the track. This fact was also noticed in [1], where a reversed time (or distance) solution was presented for a special case of curves (Euler spirals). Here a more general forward solution that is implementable in causal time and handles a more general class of curves and tracks was aimed at. It should be clear from the discussion above that the information about the tracks curvature in front of the vehicle is a necessity to be able to respect the velocity limits determined by the curvatures of the path.

The path preview information is the most important task for calculating the limit velocity as indicated above. This determines the distance before which braking has to be initiated such that the vehicle can slow down to the target velocity given by (3.3). If the preview distance specified is too large, then there is a risk of conservatism, i.e. a vehicle that brakes too early and not utilizing its capability. On the other hand if it is too small the braking may be initiated too late thus leading to the vehicle going off-track. The specific preview distance/time is, without a priori information about the track's topology, a tuning parameter to ensure remaining on track and yet be close to the limit and high performance.

This thesis presents two approaches that use preview information about the curve radius as the a priori information about the track and the user inputs of acceleration limits to compute a longitudinal velocity profile. The first one uses one single preview point to determine the decision of braking or acceleration while the other approach uses multiple preview points to achieve a potentially higher performance.

3.3 The single-point preview strategy

This strategy employs a very simple approach for the look-ahead distance. Time to brake from the current vehicle velocity, v_x to a complete standstill is calculated. It is also assumed full braking is done every time meaning a constant value of deceleration is assumed. According to Newton's second law, the relationship for distance travelled by a body travelling with a velocity v_x, decelerating constantly at the rate of $a_{x,max}$ and coming to a standstill is

$$s = \frac{1}{2}\left(\frac{v_x^2}{a_{x,max}}\right) \tag{3.4}$$

Here s represents the distance at the end of which the next curvature of the road is calculated and subsequently the limit change of velocity is found using (3.3). In order to avoid a sliding mode solution and the numerical problems that comes with such a behaviour a numerical "relaxation" was introduced and the following equation governs the velocity profile,

$$\dot{v}_x = tanh(K(\sqrt{R_s a_{y,max}} - v_x))a_{x,max}\sqrt{1 - \left(\frac{v_x^2}{R a_{y,max}}\right)^2} \tag{3.5}$$

Where R_s is the curve radius taken at the look-ahead distance determined by (3.4) and *tanh* is the tangent hyperbolises function which implements a "soft" sign function with a tuneable slope of K. For the acceleration case, the left hand side of (3.5) is compared with the acceleration/deceleration capability of the vehicle (parameters specified by the user) and the smallest of these values determine the slope of the velocity profile.

Figure 7 shows the comparison between velocity profiles generated based on equation (2.8) and equation (3.3). When limits for braking are imposed, the ramp down in velocity from a very high value on the straight to a relatively lower finite value due to curvature change is seen. The slope of this ramp as indicated by the green line is a measure of deceleration experienced by braking. Similarly, acceleration limits need to be imposed on exits out of corners as well as on straights. The slope of the line from 0 to 100 metres quantifies the value of acceleration. After 100 metres the braking continues the deceleration of the vehicle till it reaches 150 metres after which the steady state (set point) speed according to equation (2.8) becomes true. The corner ends at 240 m and leads to a straight. Here the target velocity is calculated with acceleration limits. The ramp up after 250 m is seen and this indicates acceleration out of corner exit. The acceleration ramps up such that the friction circle is respected at all times.

It is to be noted that the preview distance plays a key role in initiating the braking. If the preview distance calculated according equation (3.4) misses a curvature for a particular track, then the distance might have shortened by multiplying with a suitable gain. Similarly, since this distance is calculated on the assumption that the braking capacity of the vehicle is constant there might be situation where the look-ahead distance might not be sufficient, for example is tight closing curve. Again in such situations the preview distance might require a bit of tuning to lengthen.

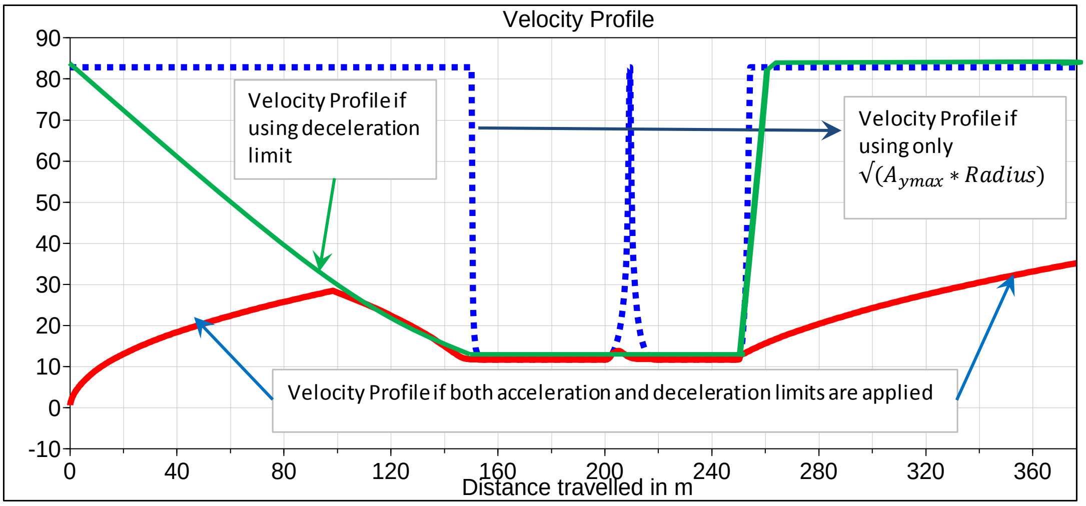

Figure 7: Velocity profile computation

3.4 Multi-point strategy:

The main disadvantage with this single point preview strategy is that it may be conservative in the sense that it brakes early resulting in a non-optimal speed calculation. Also there a situation may be encountered where there is risk of pre-mature acceleration. For example, if a short bend lies in the middle of a long straight, there is a risk, when the preview is not fine-tuned, that there might be early braking due to a large preview and a pre-mature acceleration due to an early preview at the exit of the small bend.

In order to overcome this potential conservatism the **multi-point preview strategy** was developed. This strategy uses several preview points to determine a more optimal braking point. For each preview point an upper velocity limit is calculated using (2.8), forming snapshots of the speed limits to come, see Figure 8.

At the current position, the acceleration capability is computed using (3.3). This capability is assumed to be constant (or increase in magnitude) during the preview horizon implying that the estimated speed ahead of the vehicle during braking is easily computed (red line in Figure 8). By comparing the estimated future velocities with the speed limits given in the preview points, a condition for all preview points can be made to determine an appropriate braking point.

The condition is:

$$v_{limit,n}^2 - v_{max,n}^2 \leq 2a_{x,n}s_n \tag{3.6}$$

Where, $v_{limit,n}$ is the predicted velocity at a point *n* in the future calculated by integration of (3.3), $v_{max,n}$ is the upper velocity limit calculated using equation (2.8)), $a_{x,n}$, again the acceleration/deceleration potential predicted using (3.3) s_n, is the distance to point *n* on the preview horizon.

The above condition verifies whether the velocity prediction satisfies Newton's second law of motion to ensure vehicle stability.

If the vehicle is travelling with a velocity $v_{limit,n}$ decelerates with a magnitude $a_{x,n}$ over a distance s_n then if it attains a new velocity which is lesser than or equal to (ideally equal to)$v_{max,n}$, which is the upper velocity limit for that point, then it implies that velocity prediction is correct.

This forms a basis to decide whether to accelerate or decelerate. If the above condition holds then vehicle is made to accelerate with a magnitude a_x calculated using equation (3.3), in which $+a_{x,max}$represents the maximum longitudinal acceleration capability of the vehicle, input by the user.

In case the above condition fails, then it implies that the vehicle needs to decelerate until equation (3.6) becomes true again. Deceleration is again calculated according to equation (3.3), with $-a_{x,max}$representing the deceleration capability of the vehicle, input by the user. This can be seen as a pictorial representation in Figure 8. If there are 3 preview points but the condition stated in (3.6) fails for preview point 2, represented by the red-line, then vehicle is made to decelerate.

In order to prevent a sliding mode solution and the numerical difficulties associated with it, a hysteresis function was added on the braking condition.

It must be noted that optimal braking time, as a consequence of the discretization of preview, will be missed by the distance/time gap between the preview points, like a quantisation error. The time/distance to the preview points may be determined using (3.4) and additional points distributed before and after or specified manually.

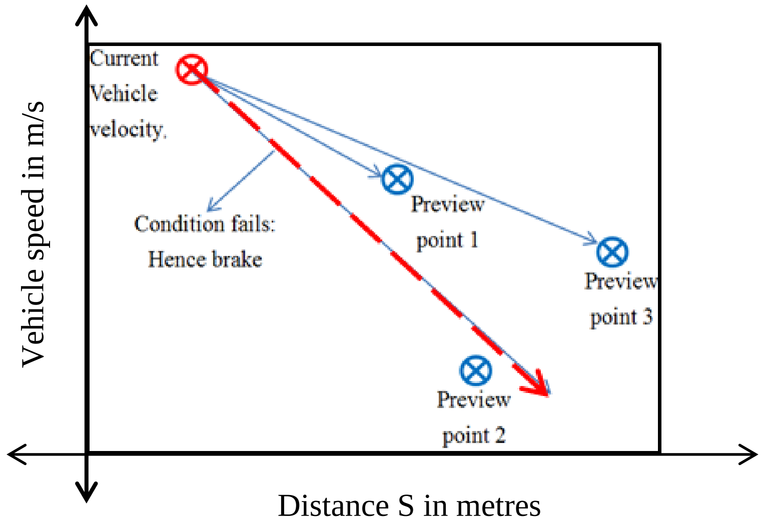

Figure 8: Evaluate $v_{limit,n}^2 - v_{max}^2 < 2a_{x,n}s_n$ at all preview points

3.5 Implementation in VDL:

The two strategies mentioned above were implemented in Dymola using VDL. This was called the Velocity planning block, layout of which is can be seen in Figure 9. It's composed of the following components:

i) Preview Distance Calculator: For the single point strategy, the preview distance is calculated using equation (3.4). For the multi-point strategy, same formulation could be used, with a number of preview points on either side of the preview from the single point strategy. The input for this block is the information about the current vehicle position which comes from perception functionality.

ii) Path Curvature: VDL provides numerous blocks to estimate the path curvature at any point on the track. Unfortunately this only works if the path is defined as centre of the road. The information about the preview points is fed into these blocks to find out the curvature. This was an implementation of an existing function within the VDL.

iii) User inputs: The user is required to input 3 values; longitudinal acceleration, longitudinal deceleration and lateral acceleration.

iv) Maximum Velocity calculation VyMax: Using equation (2.8) and the user input for maximum lateral acceleration, the threshold limit for speed on any point on the track is estimated.

v) Estimation of limit velocity: Output of all the above mentioned quantities are input into the block depicted as 'limitAcc' in Figure 9. Depending on whether the single point or the multi-point preview strategy is used, the inputs are then used to integrate Equation (3.3), the result of which is an estimated velocity.

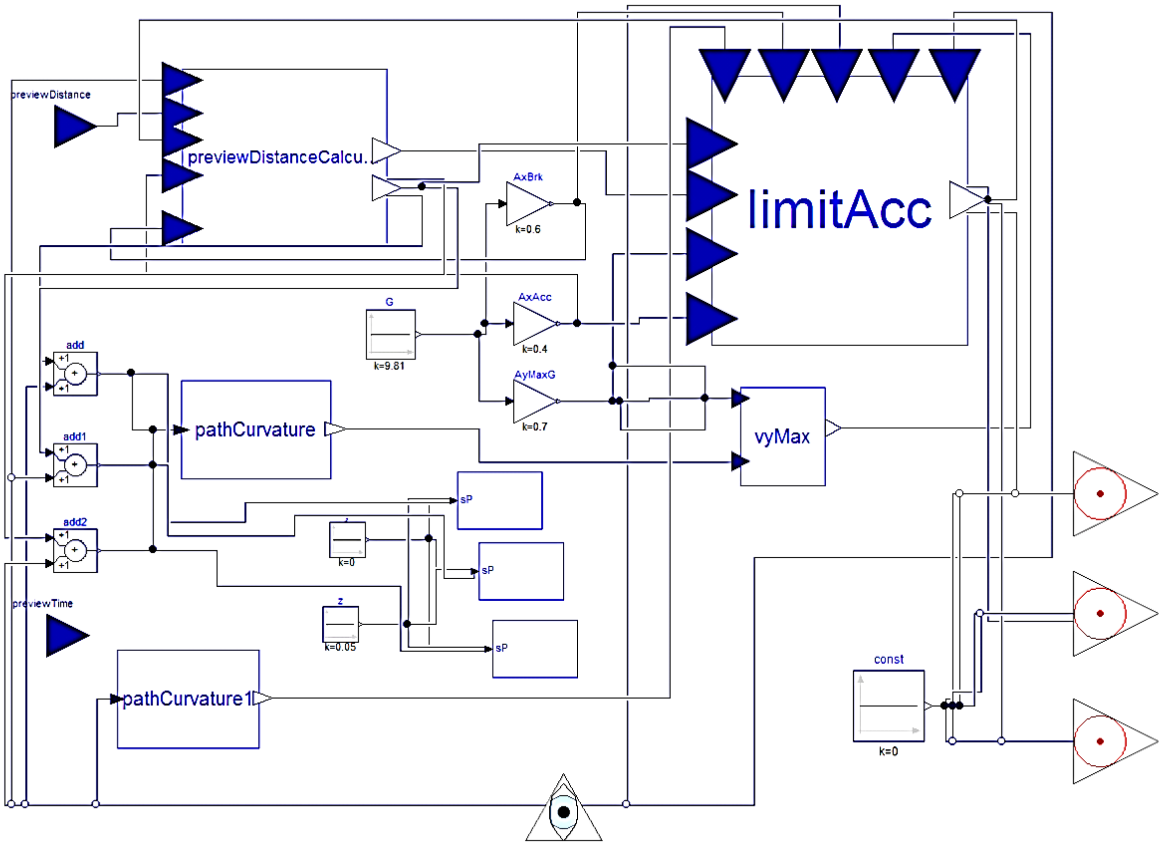

Figure 9: Velocity planning block

This estimated velocity is then input into to the existing longitudinal controller of the driver model. The VDL driver model has three main controllers that are in charge of longitudinal propulsion:

1) Longitudinal tracker:
2) Gear selector
3) Gear shifter

The longitudinal tracker is a PID controller, which compares the difference between the current vehicle speed and that of the reference speed it receives from the velocity planner. Accordingly it translates the difference, if negative, as a force demand on the brake pedal, otherwise as normalized position of the accelerator pedal. It also receives feedback from the current brake and accelerator positions. This controller directly operates the brake robot, while the normalized accelerator command is output to the Gear shifter. This PID controller is tuneable; details of all the gains set are mentioned in section 4.1.

The gear selector also gets the input of the current vehicle velocity compares it to the reference velocity. Based on this comparison, it selects one among 3 modes, which, are cruising, accelerating or retarding. Centred on this decision, it compares with either an engine map (rpm based selection) or map relating vehicle speeds (speed based selection) and generates an output of the appropriate gear to be selected.

The gear shifter block, based on the input it receives from the above stated blocks, controls the clutch, accelerator and the gear robot.

The lateral control of the vehicle is controlled by a steering controller, which was developed in [9]. It measures the error between the current position of the vehicle and the reference path as well as the error between the estimated position of the vehicle in the preview horizon and the reference path and acts in such that this error is kept to a minimum. This controller translates the error into a steering wheel angle on the steering robot that ultimately steers the vehicle.

Figure 10 shows the scheme of the complete driver model.

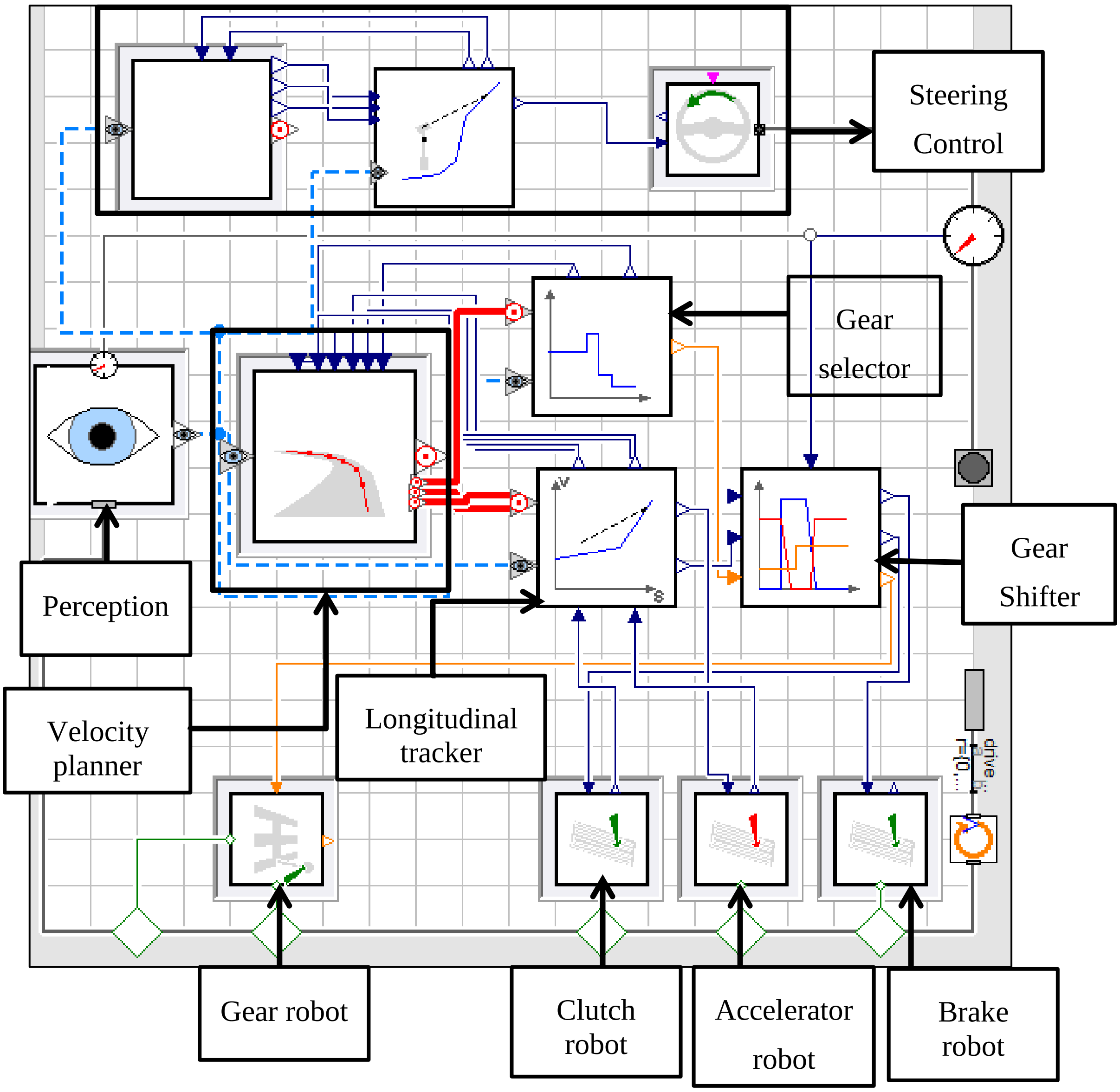

Figure 10: Complete Driver Model

4 Results

Extensive simulations were conducted using the single point tracker on two vehicles from the VDL. The VDL consists of many chassis and sub-systems and using the same a Formula SAE vehicle was assembled. A pre-defined compact car from VDL was the other vehicle that was used. Limited trails were conducted on the multi-point tracker due to shortage of time, the results for which are presented at the end of the section.

4.1 Vehicle models used and specifications:

1) Formula SAE open wheel race prototype model:
   Double wish-bone suspension setup with Pacejka 2002 tyre model, basic hydraulic brakes and a rear Wheel driveline
   - Wheelbase: 1.65 m
   - Front track width: 1.29 m
   - Rear track width: 1.2 m
   - Mass :200 kg
   - Roll Moment of Inertia : $I_{xx} = 30$ kgm^2
   - $I_{ZZ} = 130$ kgm^2
   - Weight distribution: 46/54 Front: Rear

The vehicle's approximate boundary limits are required as input for the velocity planner. A few simple open loop manoeuvres were performed and the following values were determined: (1 g = 9.81 m/s^2)

- Longitudinal Acceleration limit: 0.4 g
- Lateral Acceleration limit: 0.8 g
- Longitudinal Braking limit: 0.7 g

2) Compact car with Elasto-kinematic suspension and Pacejka 2002 tyre model, Front Wheel driveline
   - Wheelbase: 2.47 m
   - Front track width: 1.4 m
   - Rear track width: 1.4 m
   - Mass :1100 kg
   - Roll Moment of Inertia : $I_{xx} = 600$ kgm^2
   - $I_{ZZ} = 1300$ kgm^2
   - Weight distribution: 63/37 Front: Rear

Approximate handling limits:

- Longitudinal Acceleration limit: 0.25 g
- Lateral Acceleration limit: 0.6 g
- Longitudinal Braking limit: 0.7 g

4.2 Track geometry:

To test the robustness of the implementation of the model, the model was tested on 4 different test tracks as shown in the table below:

1) Extended chicane:
   This track resembles a chicane on a typical race circuit. This is often found at the end of a straight line or a high-speed corner, followed by a sharp left-hand (LH) curve and right-hand (RH) curve. This tests the ability to brake from a very high speed to a low-sheep sharp turn. It tests the transient cornering ability of the vehicle during the LH and RH turns which involves load transfer on all wheels. The sharp turns are followed up a by straight or high speed curve to test the acceleration capability of the driver. The quickest driver is the one that manages to put the power down earliest and still not spin the wheels or loose traction out of the corner.

   Specification of the track as follows:

   - Length of the entry straight - 150 m
   - Length of the exit straight - 70 m
   - Radius of LH turn - 20 m
   - Radius of RH turn – 20 m

2) Circle:
   This 2-D track has a constant radius of 50 m. It must be noted that it has no-banking. This simply tests the stability of the vehicle and the performance of the lateral and longitudinal controller to accurately track the path velocity and curvature as defined.

3) High speed J-turn:
   This track consists of a long straight leading into a curve of a large constant radius. This is meant to test the ability to brake from a high speed but at the same time carry the velocity onto a high speed curve. The length of the entry straight is 300 m while the radius of the curve is
   80 m.

4) Clothoid-Hairpin curve:
   A Clothoid is a curve whose curvature changes linearly as the distance increases. A hairpin curve was modelled using the Clothoid function. This resulted in an entry straight of 100 m leading to curve whose radius decreases linearly to a value of 16.667 m over a distance of 50 m and increases back to a straight line over 50 m again. This track test the numerical stability of the implementation of equations stated in section 3.1 and is a test of robustness of the model.

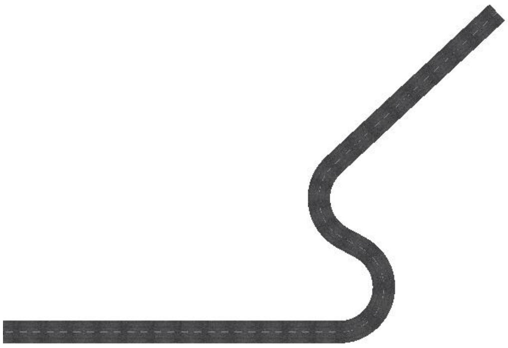

Figure 11: Extended chicane

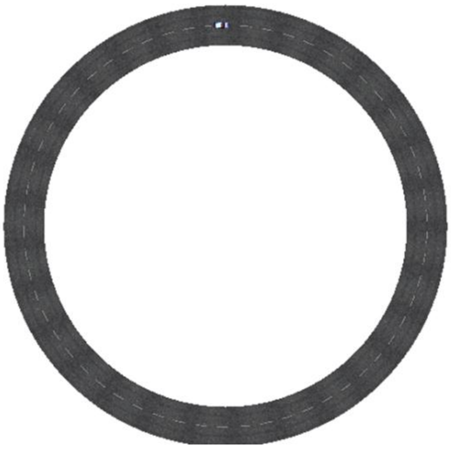

Figure 12: Oval (no banking)

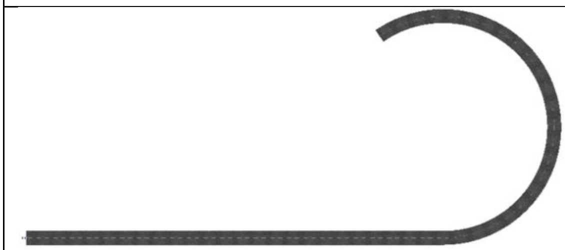

Figure 13: J-turn

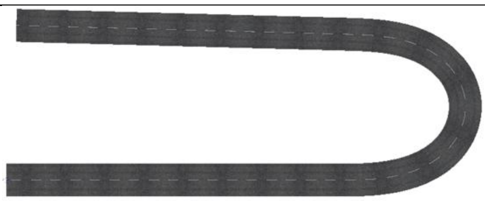

Figure 14: Clothoid - Hairpin curve

The vehicle parameters were input in the velocity planning block as shown in the Figure 9. The FSAE racer prototype model was assemble using different subsystems from the Vehicle dynamics library. Mass of this model was 200 kg which considerable less than the other vehicle models pre-defined in the library. So it is understandable that the longitudinal controller, whose gains seem reasonable for the other vehicle models, needed some fine tuning. This was done iteratively as the performance on a circuit was analysed.

The most challenging among all the tracks mentioned above was the extended chicane and the PID gains were tuned for this circuit. These gains work well for all the other circuits as well. The original parameters of the controller were employed for the compact car while the modified gains of the PID used for the FSAE racer. *See* Table 5.1

4.3 Performance evaluation on FSAE race prototype model

4.3.1 Extended Chicane

- **Velocity tracking**

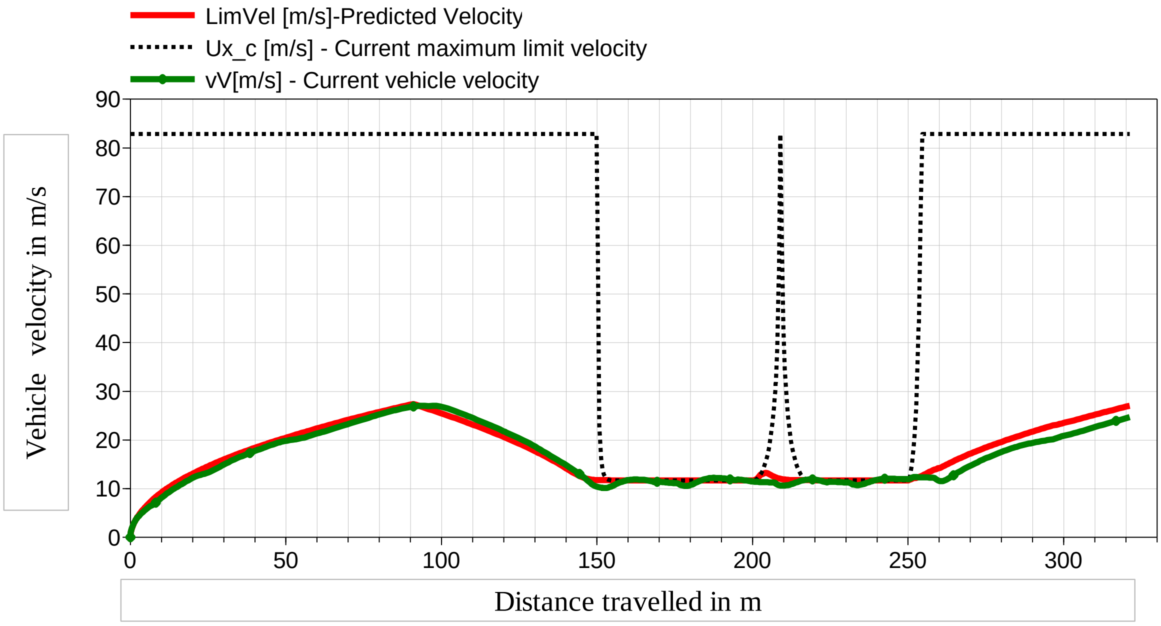

Figure 15: Velocity profile and Vehicle velocity - Extended chicane

The velocity profile generated the velocity planning block and the velocity tracked by the vehicle is shown above.

The "Predicted velocity" is the output of the velocity planning block. It is the result of applying acceleration and deceleration limits on the maximum curvature velocity as shown by the dotted line (given by equation (2.8)).

It is seen that till a distance of 90 m, the vehicle accelerates, as the input it receives is that of an increasing velocity profile that has a slope of approximately 0.4. This corresponds to the acceleration limit of 0.4 g specified by the user in the velocity planning block.

At the same time, the look-ahead point is seen to be calculating the limit velocity on the curve ahead by distance calculated according to (3.4). As mentioned earlier, this look-ahead or preview distance represents the distance needed to come to a complete standstill from the current speed with which the vehicle is travelling. In this case, the maximum braking capacity is input by the user as 0.6 g.

Therefore after having travelled 90 m on the track, the preview velocity, looking ahead at a distance of 150 m, observes that the current predicted velocity is greater than maximum curvature velocity. This initiates braking with maximum capacity of 0.6 g. The velocity planning block calculates a reduction in the predicted velocity around this set point value according to equation (3.5) with a slope of approximately 0.6. It can be seen that both the acceleration and deceleration follow the form of a curve rather than a straight line. That is because equation (3.5) is designed to model the boundary of an ellipse, to be more precise, the friction ellipse.

This directly translates into braking initiated by the vehicle, resulting in a deceleration close to 0.6 g. Thus between 90 m and 150 m, vehicle velocity is reduced with an approximate slope of 0.6. This process continues till the set point velocity for the curvature is reached (again calculated equation (2.8)) after 150 m. At this point equation (3.5) becomes zero as the vehicle velocity approaches the maximum curvature limit velocity Ux_c. Thus the output of the velocity planning block continues to be the set the point velocity. There is a small spike in the centre , when the LH curve changes into a RH curve, and at this point a small acceleration is experienced, which when integrated, doesn't result in any significant change in the velocity. The longitudinal controller manipulates the throttle, gear selection, clutch and the brake and tries to follow this constant velocity input. It is seen that the limit velocity on the curves is followed rather well for the distance between 150 and 250 m.

After 250 m, the curvature ends and the straight line section begins immediately. This marks the corner exit section. There is a step increasing in the limit curvature velocity as can be seen from the sharp jump in the dotted line. This is seen by the preview point which initiates acceleration again calculated at 0.4 g again using equation (3.5). The vehicle velocity follows this input reasonably well, except upon exit there is a slight dip in velocity when it just exits the corner. Further analysis is done by studying the friction utilized by the tyres and the driving robot performance.

- **Tyre-Friction Utilized**

One of the ways to verify whether the vehicle is being pushed to the limits of performance is to plot the normalized tyre forces. The above figure shows the plot of longitudinal force F_x and the lateral force F_y at the tyre divided by the normal load F_z on the tyre. This gives a measure of the friction utilized by the tyre.

Since this is a rear wheel driven car, the rear tyre slip during the initial acceleration of the vehicle was seen to large. As indicated in Figure **17** , the rear axle is completely utilized during the first 90 m (straight line acceleration).

Between 90 m and 150 m, where deceleration occurs, it is seen that the friction utilized at the front axle increases to 50 % due to the effect of weight transfer under braking, while at the rear driven axle friction levels average around 80 %.

During the LH the curve the non-driven front axle is utilized to around 80 %, as it undergoes lateral slip resulting from the steering input. The rear left tyre, which is the inside wheel, is exhausted during the LH curve (150 – 200 m) due to combined lateral and longitudinal slip. Similarly, the rear right tyre gets completely utilized in the RH curve (200-250 m). The rear axle thus is seen be the limiting factor for the limit of lateral acceleration achievable. Initially it was set to 0.8 g, for which the rear driven axle drifts out on the corner exit (at 250 m). Subsequently the lateral acceleration limit for which the vehicle was seen to be stable was for a value of 0.7 g.

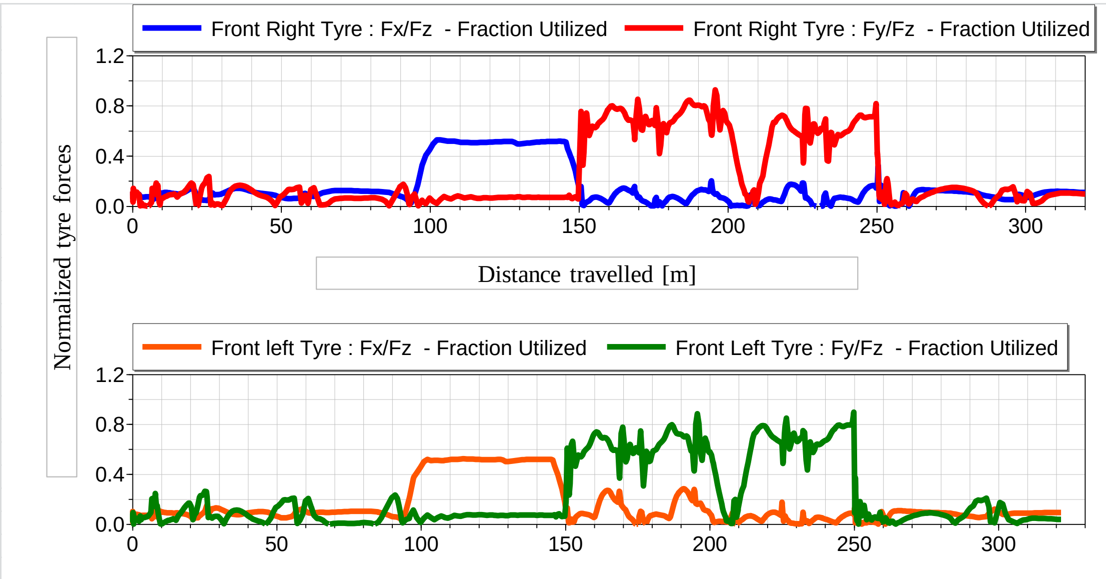

Figure 16: Tyre Friction utilized - Front Axle

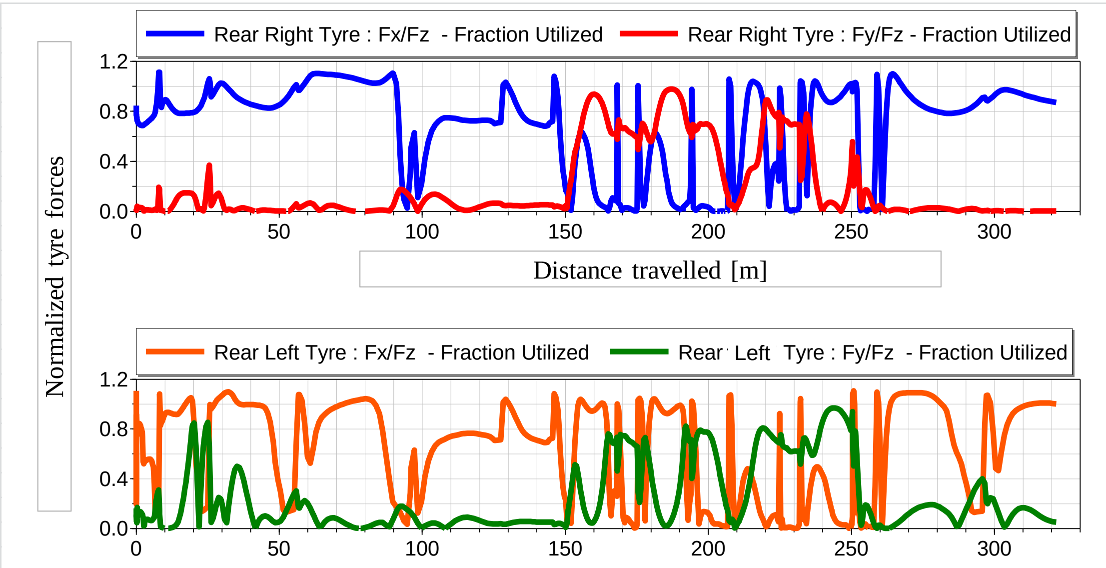

Figure 17: Tyre Friction utilized - Rear Axle

- **Longitudinal control of the vehicle**

It is seen that the longitudinal controller operates at full throttle on the straights between (0-90 m) with gear shifting sequentially increasing from 0 to 5, *See* Figure 18. This results in the constant increase in the speed of the vehicle. When the deceleration signal is received, maximum braking is initiated.

At this point the vehicle enters the curvature of (constant radius) and receives an input to track a constant velocity value. It is seen that the controller applies the throttle and brake alternatively to keep the vehicle as close as possible to predicted velocity.

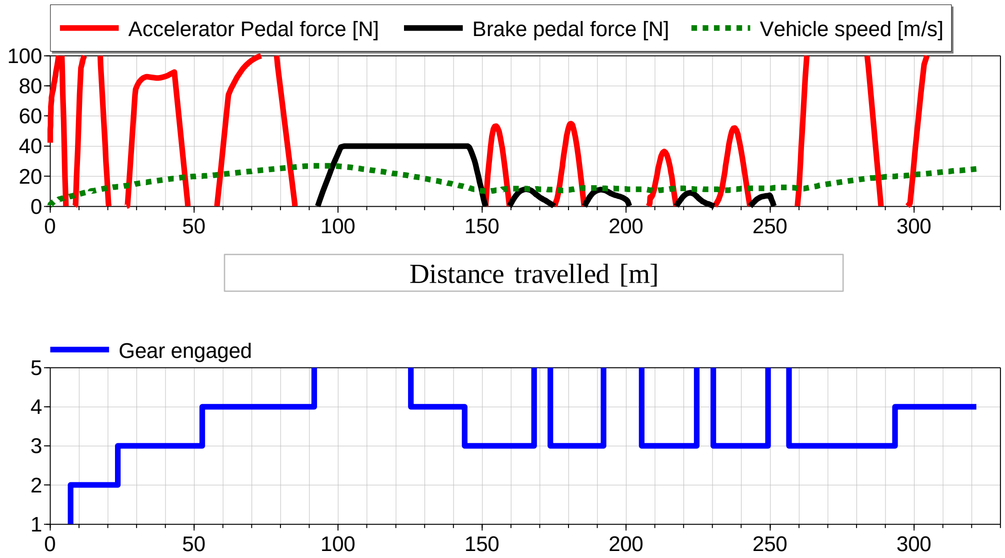

Figure 18: Control actions indicated by the driving (throttle, gear, brake) robot over the velocity range

It is observed that the gear-shifting is not optimized. It is quite noticeable that when travelling through the LH and RH curves (between 170-250 m) that whenever the brake is applied, the gear shifting is also actuated and thus the 5th gear gets engaged repeatedly which ideally is not desirable.

Also the maximum allowable braking force was kept to 40N and thus this value, as seen in the figure represents maximum braking, consequently resulting in a deceleration equivalent to 0.6 g. The reason was to limit the braking force to 40N from a default value of 500N was to take into account the weight difference when this vehicle is compared to other standard vehicles used in VDL. The vehicle, weighing in at just 200 kg is around 5 times lighter.

- **G-G plot**

The G-G plot as described in section 2.4 provides a measure for performance of the driver. As is known, the best drivers always drive on the edge of the friction circle/ellipse [3]. Hence a plot of longitudinal acceleration v/s lateral acceleration would be beneficial to evaluate the performance of the driver model. From Figure 19, it is observed that during the straight line, the vehicle traces the centreline. It is seen it achieves an average value of 0.4 g in acceleration and 0.6 g during breaking as specified. When negotiating the curves it achieves an average value of 0.7 g while achieving a max value of 0.8 g due to a slight oversteer on corner exit.

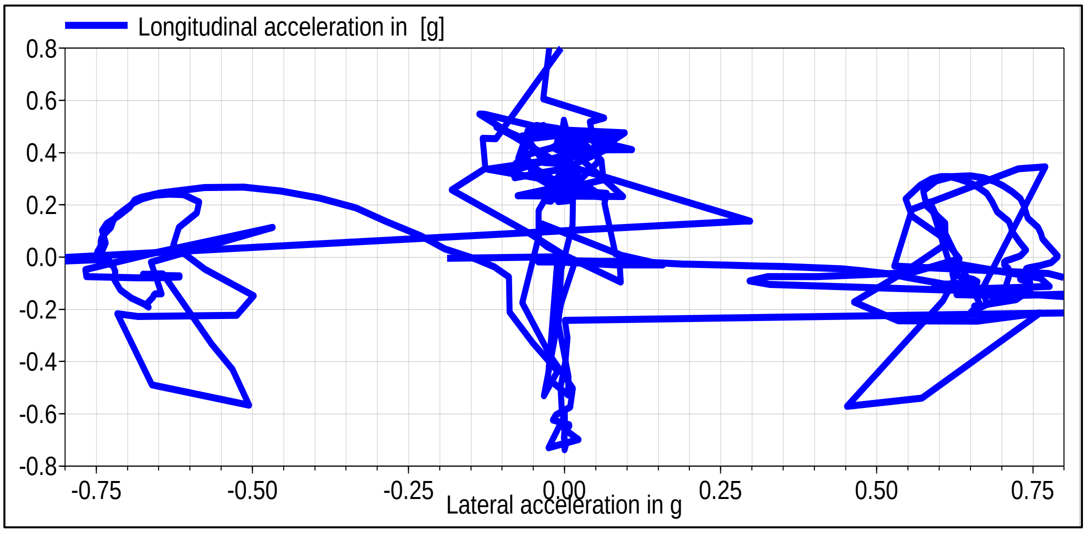

Figure 19: G-G Plot for extended chicane

4.3.2 Circle

In order to evaluate the performance of the driver model in steady-state conditions, the vehicle model was simulated on a circular track with a constant radius 50 m. The track was built using the road-builder function in VDL. Two laps were performed; hence the abscissa of all graphs for this particular track is in seconds.

- **Velocity tracking**

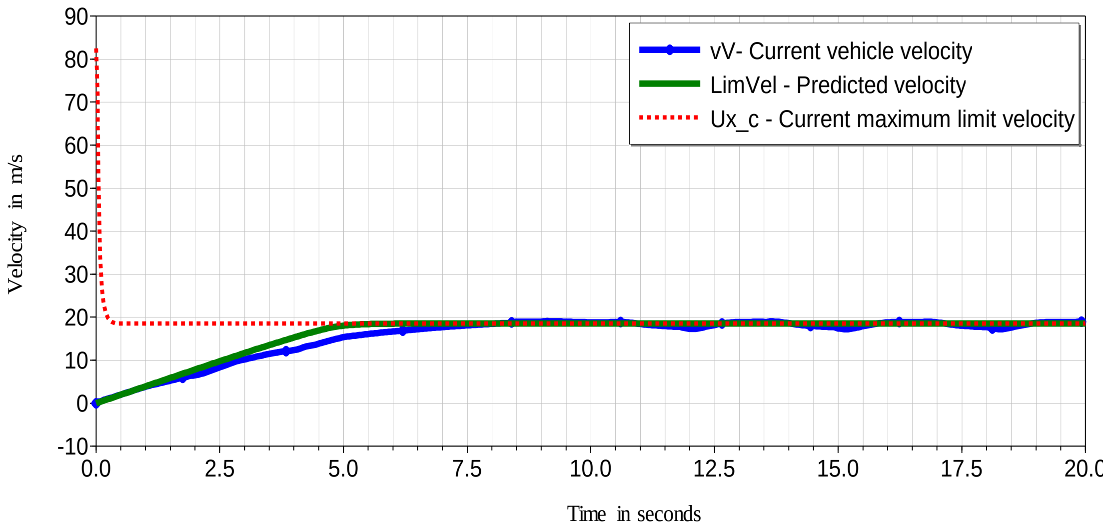

Figure 20: Velocity profile and vehicle velocity

The velocity planning block takes into account the acceleration limit of 0.4 g and takes about 5 seconds to reach the steady velocity corresponding to 0.7 g of lateral acceleration. The vehicle is seen to follow the velocity profile reasonably well but a small variation is seen after the vehicle has attained steady state velocity.

- **Tyre Friction utilized**

  The vehicle is driven in clockwise direction. Therefore the left tyre forms the inside wheel. The rear axle, as mentioned earlier is the driven axle. The front axle friction is utilized up to 80 %. It is built up gradually as the steer input increases till the set point velocity is achieved. In order to maintain the vehicle on the trajectory at this speed, the steer input is constantly corrected, which is evidently seen at the front steered axle. *See*

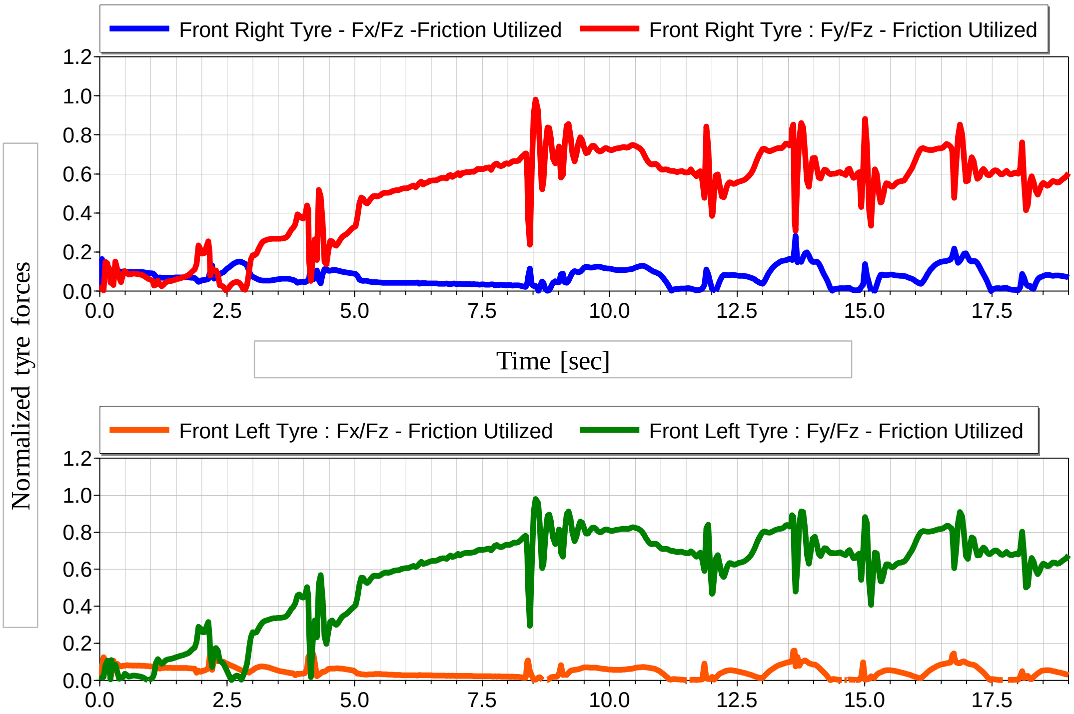

  Figure 21

  The rear driven axle is seen to be fully utilized. The Rear right tyre is the outside tyre, that spins faster than the inside rear left tyre. Hence the longitudinal slip is seen to be more. *See* Figure 22. The inside tyre is subjected to more lateral slip, resulting 90 % of the friction being utilized.

  An interesting observation is that rear right tyre, after the vehicle attains the set point velocity, is subjected alternate periods of longitudinal and lateral slip.

- **Longitudinal control of the vehicle**

  Figure 23 shows the actions of driving robot that better explains the behaviour of tyres. In order to maintain the set point velocity as well as the trajectory on the path, the longitudinal controller alternates actions on the steering as well as brakes. During the periods when the accelerator is engaged, the longitudinal slip increases, while during braking the lateral slip of the tyre increases on the rear right increases.

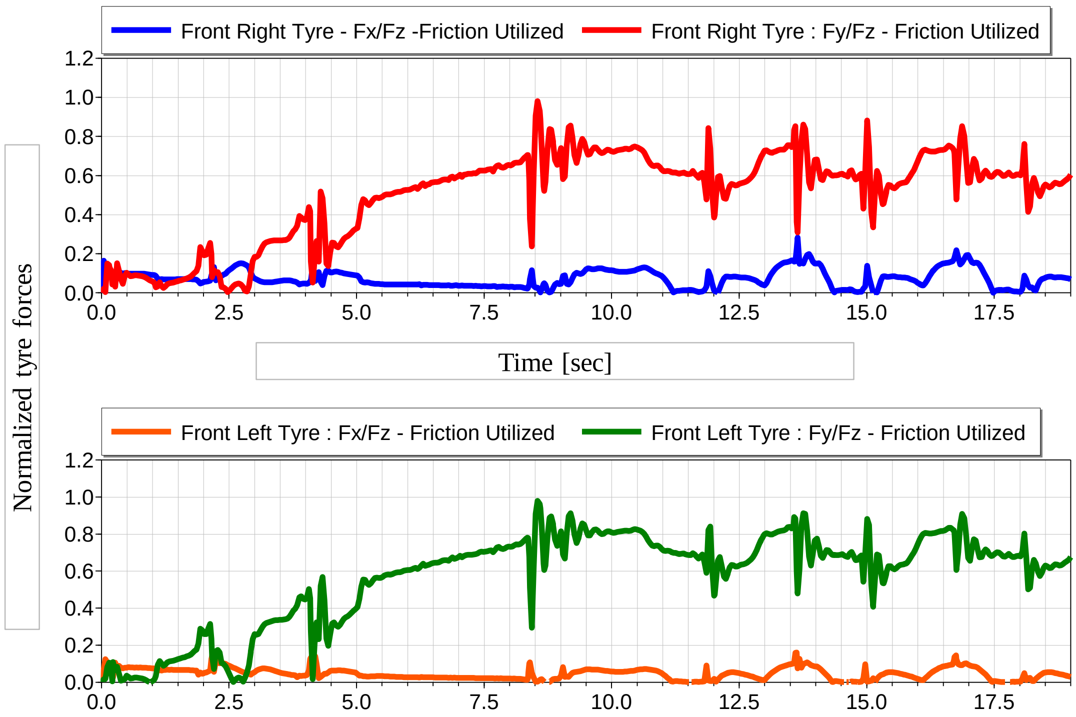

Figure 21: Tyre Friction utilized: Front axle for an Oval (2-d) track

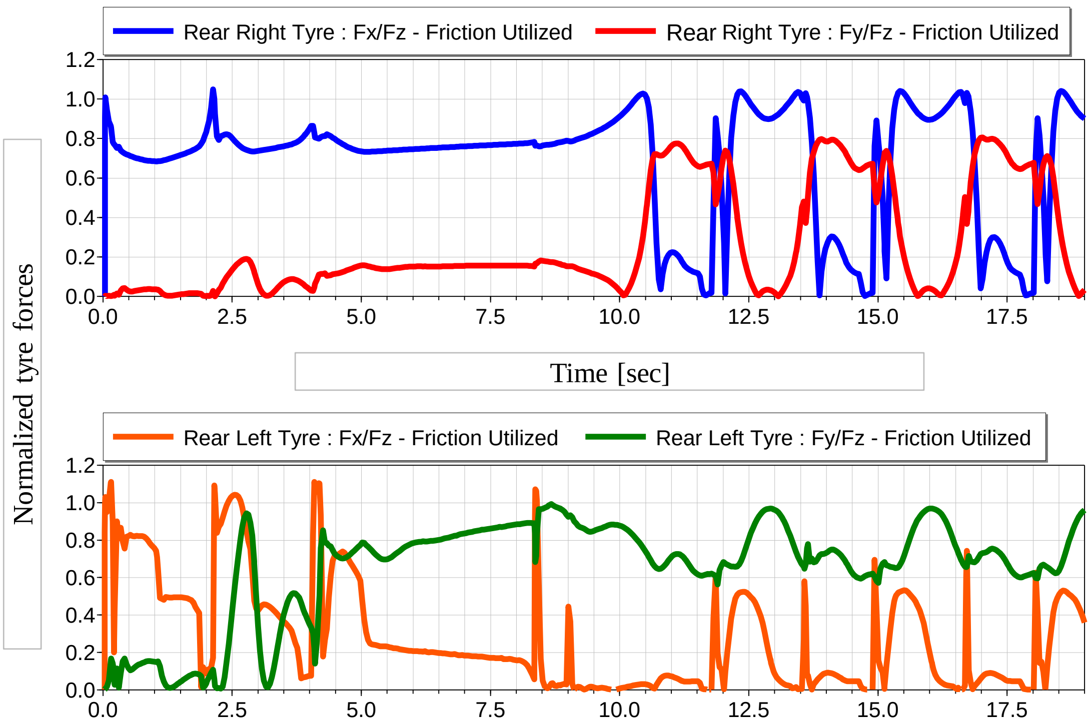

Figure 22: Tyre Friction utilized: Rear axle for an Oval (2-d) track

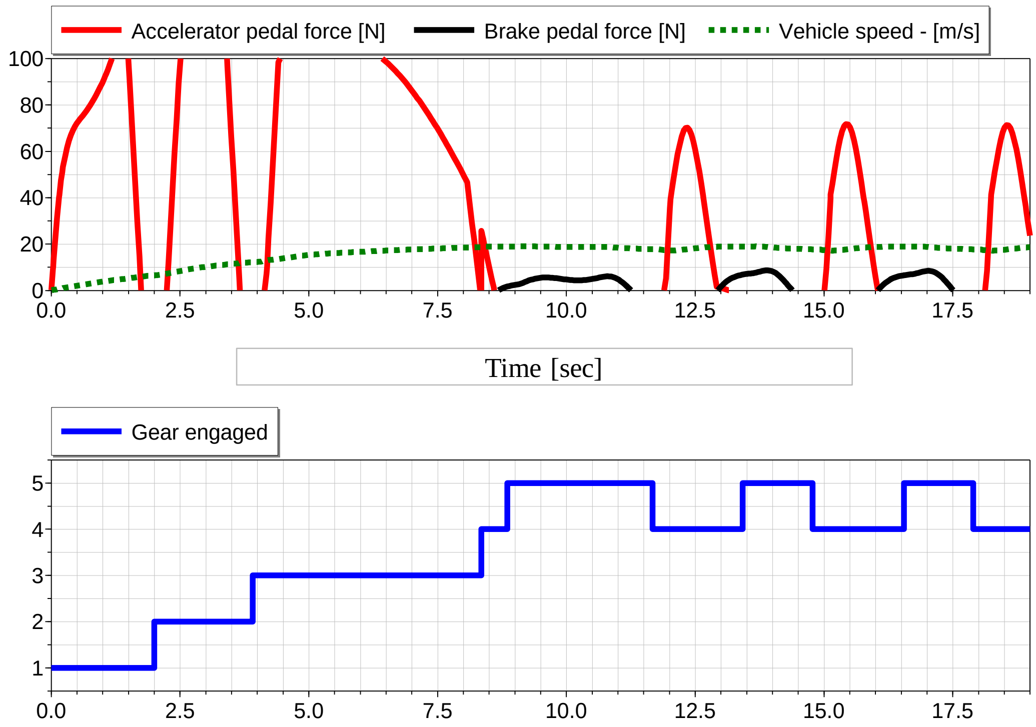

Figure 23: Control actions indicated by the driving (throttle, gear, brake) robot over the velocity range

- **G-G plot**

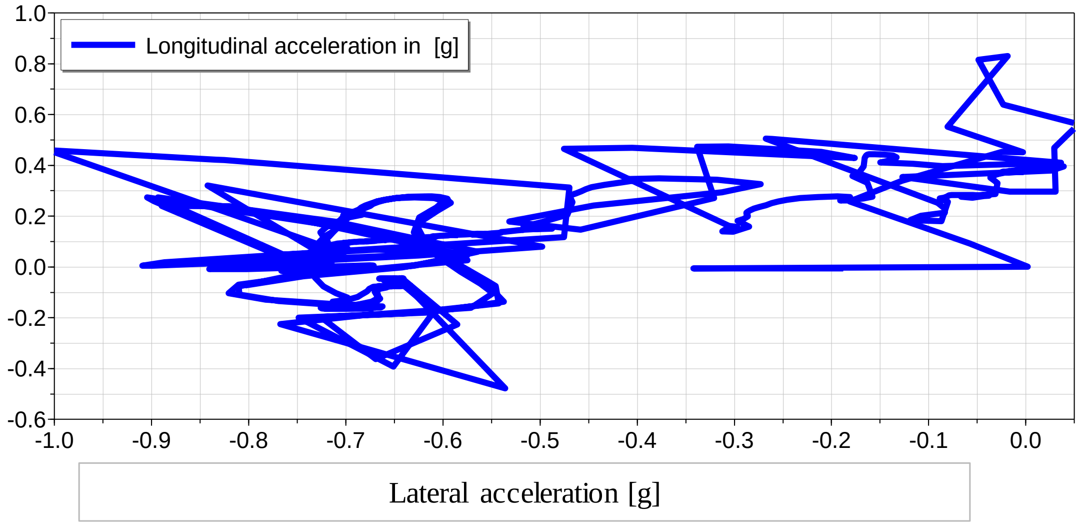

Figure 24: G-G plot for Oval (2-D) track

The G-G plot above shows, as expected, a combined effect of longitudinal and lateral acceleration. It is interesting to note that at high values of lateral acceleration of around 0.7 g, the braking action subjects the vehicle to a deceleration.

4.3.3 Hi Speed J-turn

This track tests the performance of the driver model on high speed track. The track consists of a long straight leading to a turn with a large curvature (4.2). The goal of course, is to travel as fast as possible on the straights, brake as late as possible and carry all of the speed into the turn.

- **Velocity tracking**

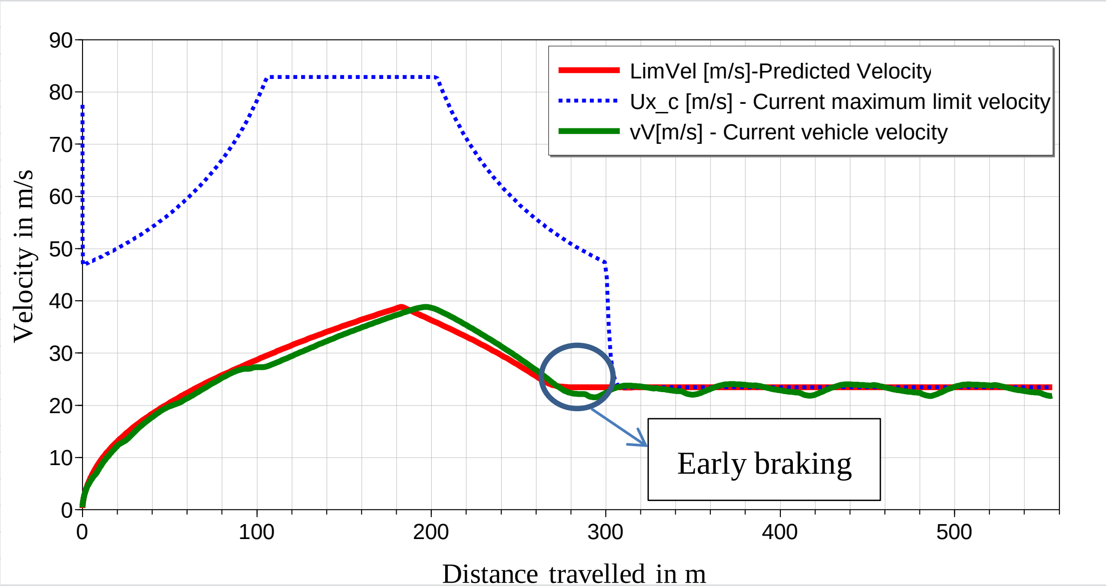

Figure 25: Velocity tracked on high speed J-turn

In this case, it is observed the velocity planner output is more on the conservative side. It is seen that the braking is performed at around 180 m from the start line. The deceleration of 0.6 g from this point leads to the vehicle reaching the set point velocity of 25 m/s for the curve nearly 30 m before the actual curve starts. This due to the fact that the preview distance is being calculated based on the presumption that the vehicle needs to come to a complete standstill from the current speed with which it is travelling in. Since the vehicle reaches a higher speed on this track compared to the previous case, the preview is longer. The preview would have been sufficient if it was calculated based on the need to decelerate from its current speed to 25 m/s, the set point velocity for the curve, instead of coming to a stand-still

This can be of course overcome by fine tuning the preview distance calculated according (3.4). But what might appear to be optimal braking for this section of the track may prove otherwise on tighter and slower section, risking going off track. This represents the compromise with the single point tracking solution.

- **Tyre-Friction utilized**

As seen in the extended chicane circuit(*see* Figure 16), the front axle being the non-driven is hardly utilized during straight line acceleration (0 m to 190 m), due to weight transfer on the rear driven axle, while under braking, around 50 % of the friction is utilized (200 m to 300 m). It can be seen on the LH turn, 80 % of the front axle is utilized *see* Figure 26 mainly due to large lateral slip cause be the steer input.

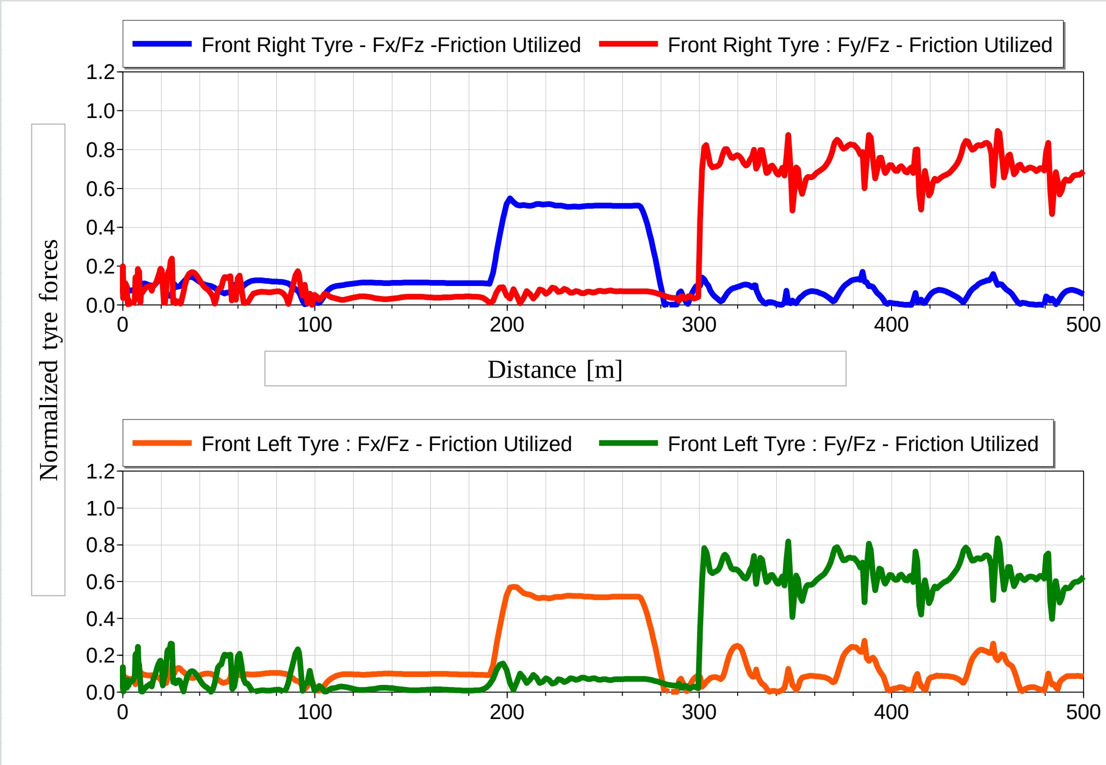

Figure 26 : Tyre Friction utilized: Front axle for an Oval (2-d) track

The rear driven axle however is completely utilized during the straight line acceleration (Figure 27) undergoing large amount longitudinal slip. During the LH turn, the inside wheel is the rear left tyre, that undergoes alternate cycles of longitudinal and lateral slip, corresponding to the alternate throttle and brake inputs (Figure 28). Rear right tyre undergoes combined lateral and longitudinal slip. The friction on the rear axle is more or less completely utilized during the LH turn, which limits the lateral acceleration levels to 0.7 g.

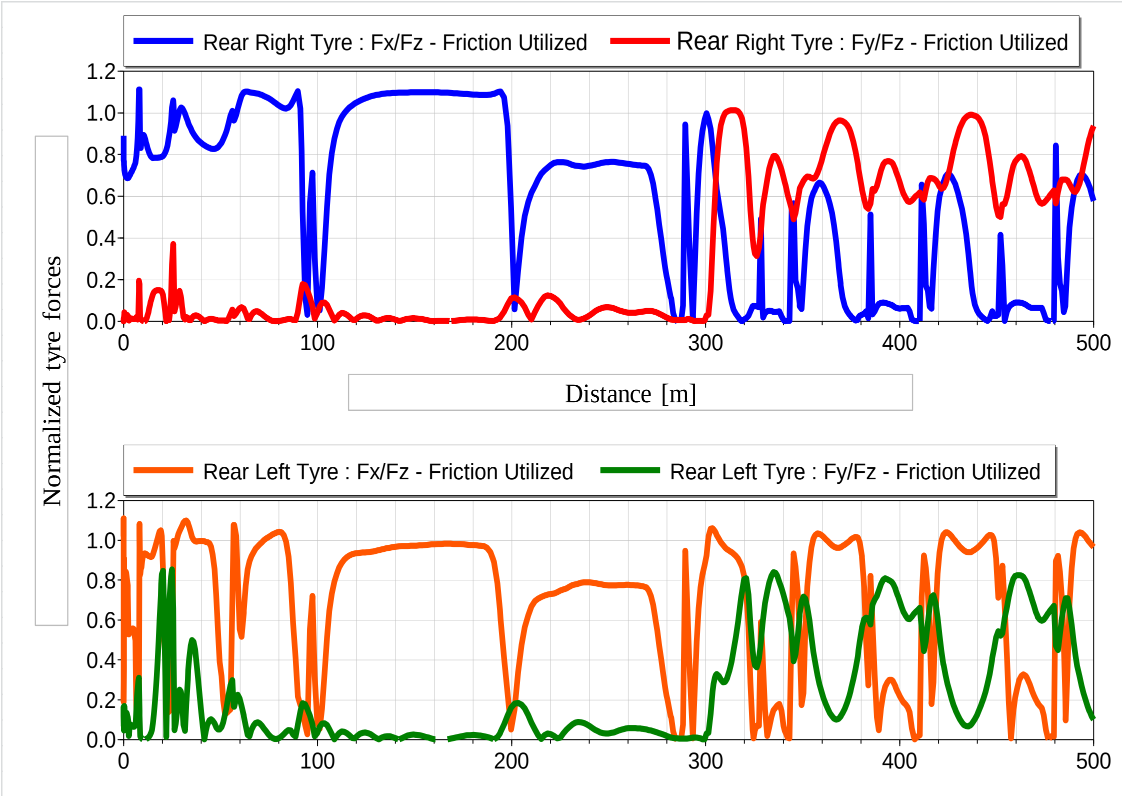

Figure 27: Tyre Friction utilized: Rear axle for an Oval (2-d) track

- **Longitudinal control of the vehicle**:

Full throttle is engaged in straight line (0-190 m), at the end of which full braking done (190-290). As seen before in the circular track (Figure 18), to maintain the target speed, partial throttle and brakes are engaged alternatively.

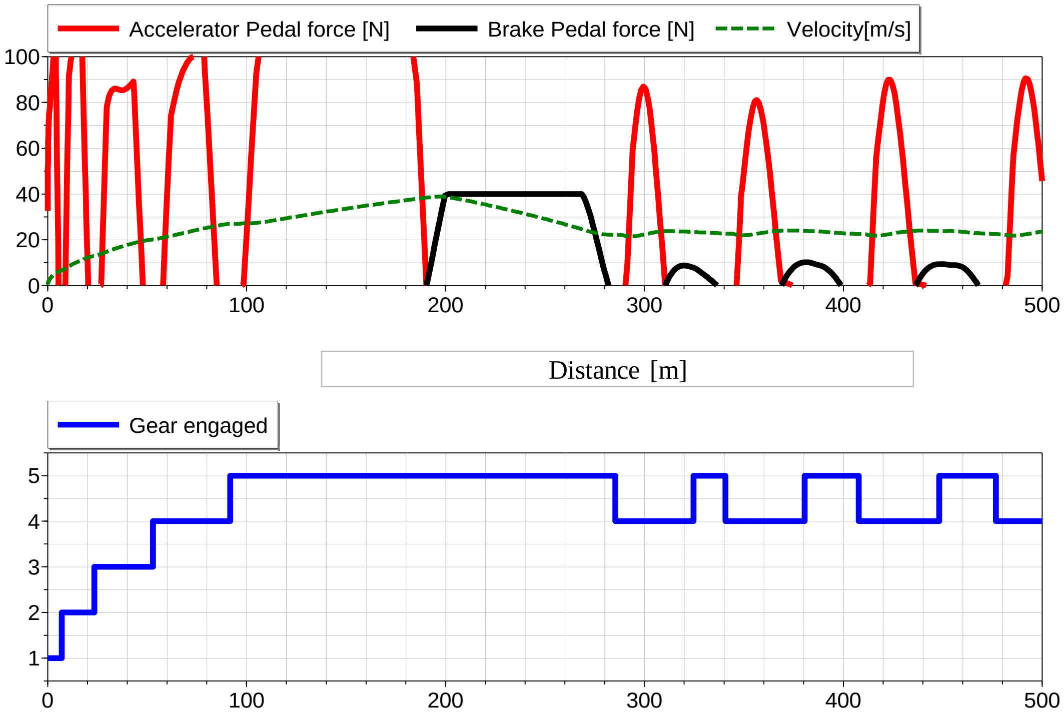

Figure 28: Control actions indicated by the driving (throttle, gear, brake) robot over the velocity range

- **G-G plot**

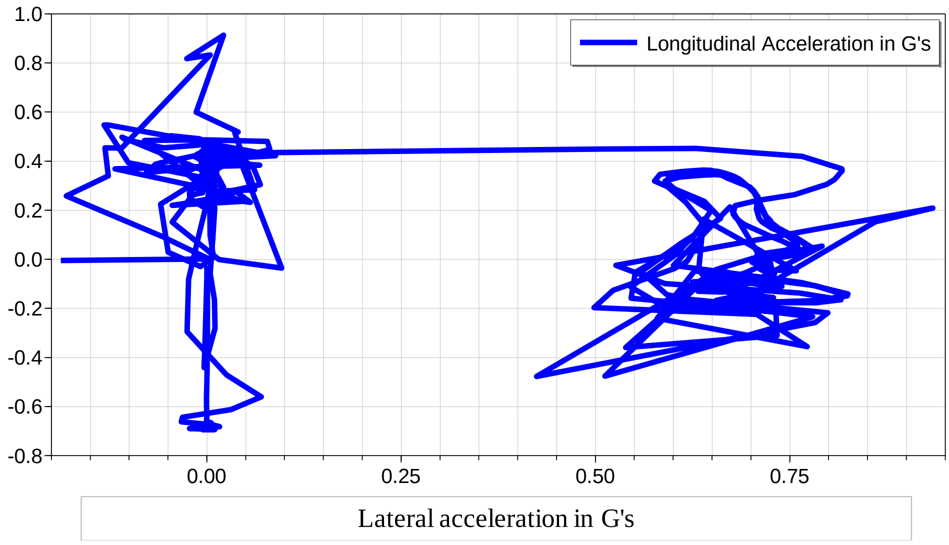

Figure 29: G-G plot for high speed J-turn

Under straight line acceleration and braking, longitudinal acceleration of 0.4 g and deceleration of 0.6 g were achieved. Values of 0.8 and 0.6 seen in the Figure 29 occurred during initial acceleration from standstill due to the large axle slip. Similarly an average value of 0.7 g in lateral acceleration was also achieved. It can be seen in the g-g diagram that for the concentration of the plots are mainly in user-specified areas

4.3.4 Clothoid-Hairpin curve:

In order to test the numerical stability of the velocity planner and the subsequent performance of the driver model, simulation on a Clothoid was performed. For this track, the curvature in the LH turn section linearly decreases with the length of the track (100 m to 150 m) and then linearly increases (150 m to 250 m) eventually leading to a straight line. Equation (3.5) lacks a solution if the radius decreases continuously. However to overcome this limitation, a lower limit of zero was imposed on the equation.

- **Velocity tracking:**

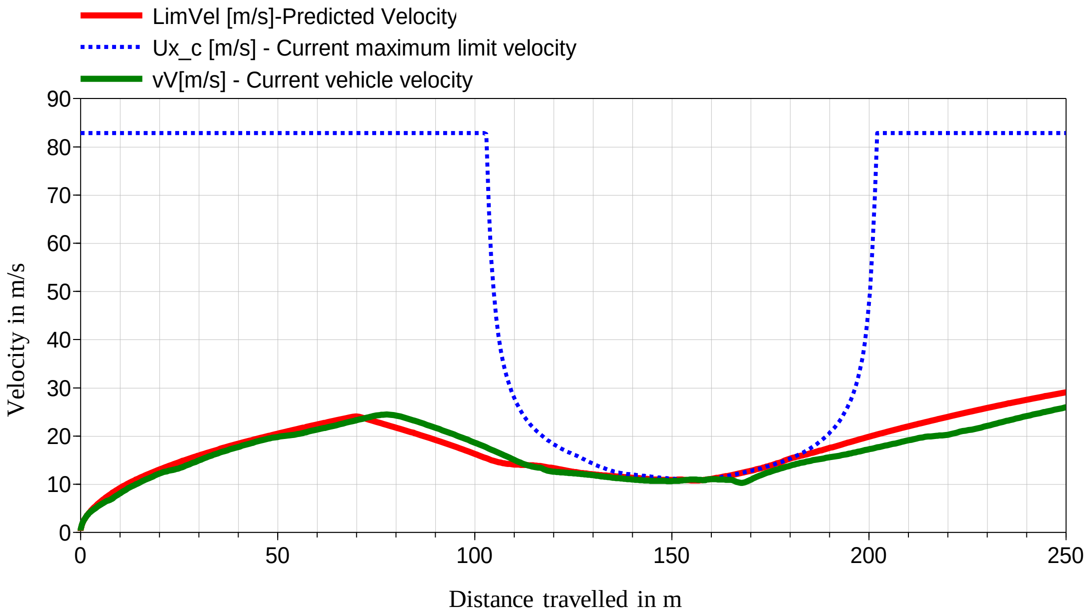

Figure 30: Velocity tracking on the Clothoid-hairpin curve

The output of the velocity block is unchanged from the previous circuits during the straight line section. The preview point is seen to look ahead until the middle of the corner (150 m) and hence initiates braking a little early at around 70 m, resulting in a deceleration. The output of the controller becomes zero momentarily (around 150 m), as the vehicle velocity becomes equal to the maximum curvature limit velocity. As the curvature increases, the current vehicle velocity eventually falls below the target, resulting in acceleration of the vehicle.

It is seen that vehicle overshoots the braking point slightly and when accelerating out of the turn, there is a slight reduction in speed. Also when exiting the corner, the rear axle is seen to break away, exhibiting oversteer behaviour.

- **Tyre-Friction utilized**

  The front non-driven axle utilizes a maximum of 80 % at mid-corner when the steer input is the largest while under braking, as seen before it is around 50 % (Figure 31).

  The rear driven axle's behaviour is similar to the previous tracks. But on the corner exit section (170 m to 200 m), as the radius of the curve increases, acceleration that the vehicle is subjected to, results in the rear axle being completely saturated. The rear left tyre being the inside wheel, undergoes longitudinal slip and is completely exhausted while the outer wheel (rear right) undergoes combined lateral and longitudinal slip, resulting in its saturation too (Figure 32). This is the cause of the oversteer on exit of the corner which eventually limits the achievable lateral acceleration.

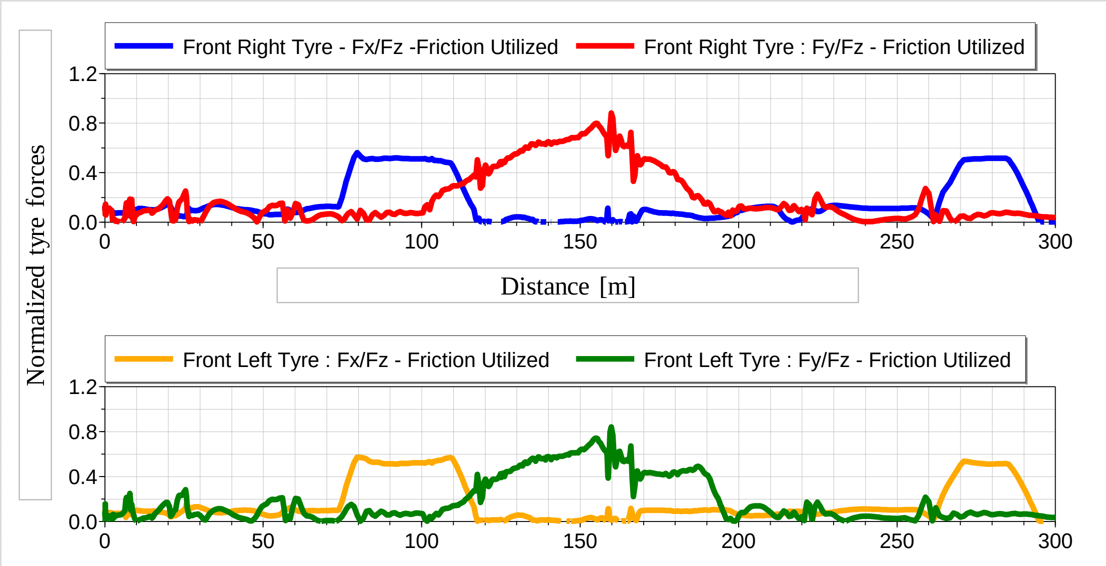

Figure 31: Tyre Friction utilized: Front axle

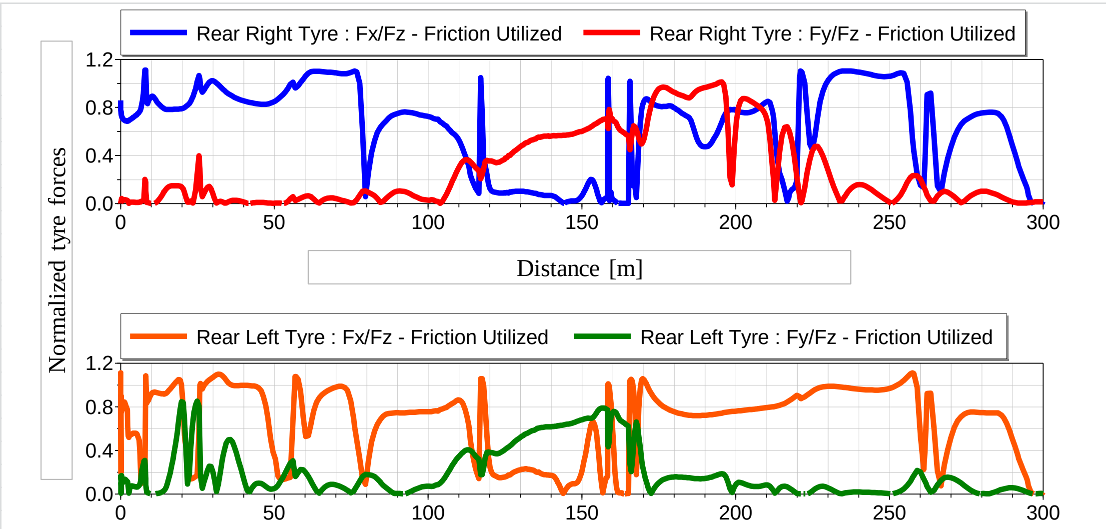

Figure 32: Tyre Friction utilized: Rear axle

- **Longitudinal control of the vehicle**

In Figure 33, 0-70 m marks the straight line acceleration section during which the vehicle is operated at full throttle. Full braking takes till 110 m. The brake gain had to be probably increased to prevent the overshoot of the braking point, although it is marginal. The gear robot unnecessarily engages top gear soon after mid-corner, which results in a dip in vehicle velocity below the target (around 160 m). This initiates full throttle, resulting in the oversteer. Please note the track runs out after 250 m and hence results seen beyond this distance are of no consequence.

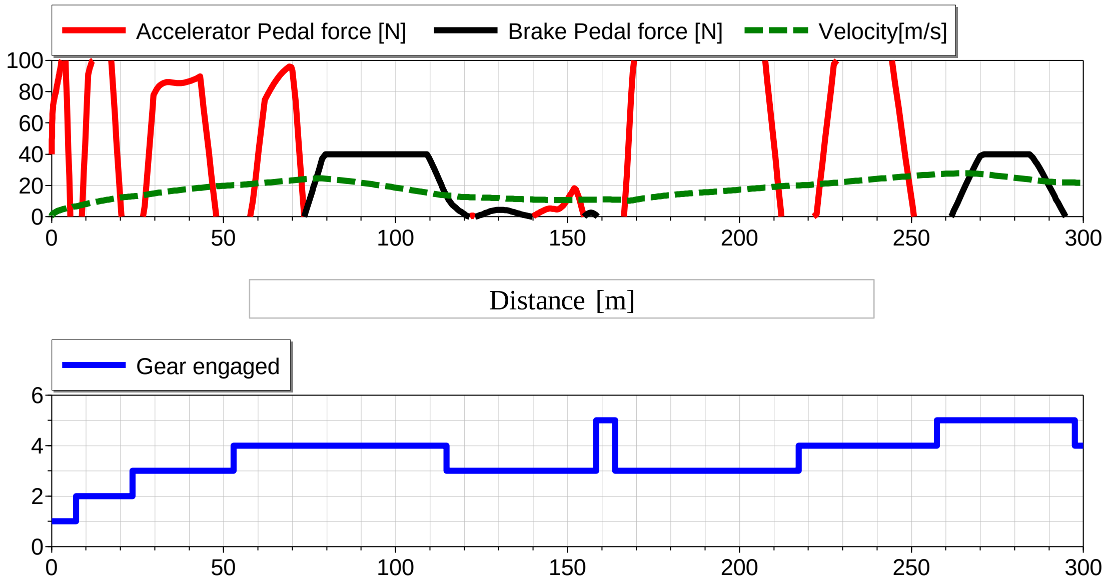

Figure 33: Control actions indicated by the driving (throttle, gear, brake) robot over the velocity range

- **G-G plot**

Figure 34 shows that the target values of longitudinal and lateral accelerations were met. The lateral acceleration gradually increases and reaches a maximum of around 0.7 g in the mid-corner region. However, the rear axle drifts out on exit. The acceleration of 0.85 g is due to this power oversteer.

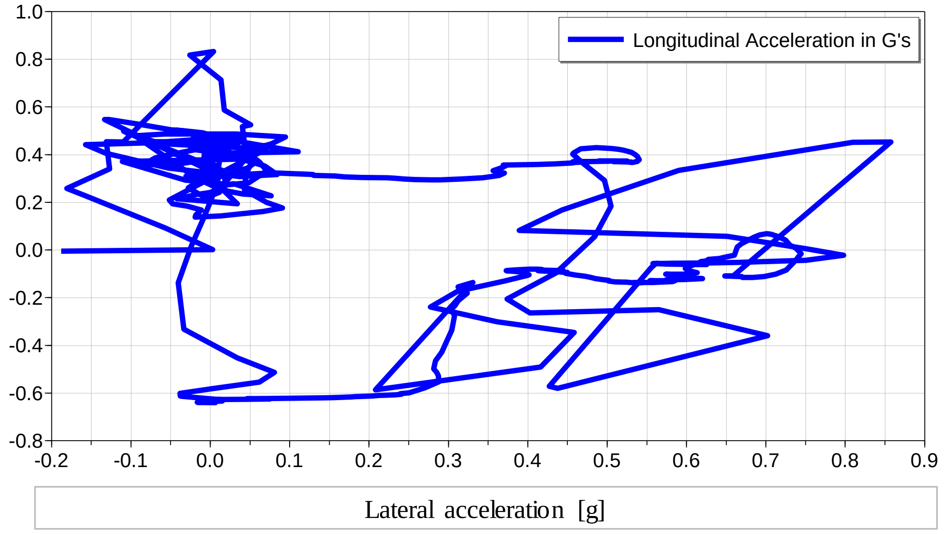

Figure 34: G-G plot for the hairpin curve

4.4 Performance evaluation on Compact Vehicle model (CompactLEKPacejka02)

To the robustness of the velocity planning block across different vehicle platforms, simulations were performed using a front wheel drive, passenger vehicle model as described earlier.

4.4.1 Extended Chicane

- **Velocity tracking**

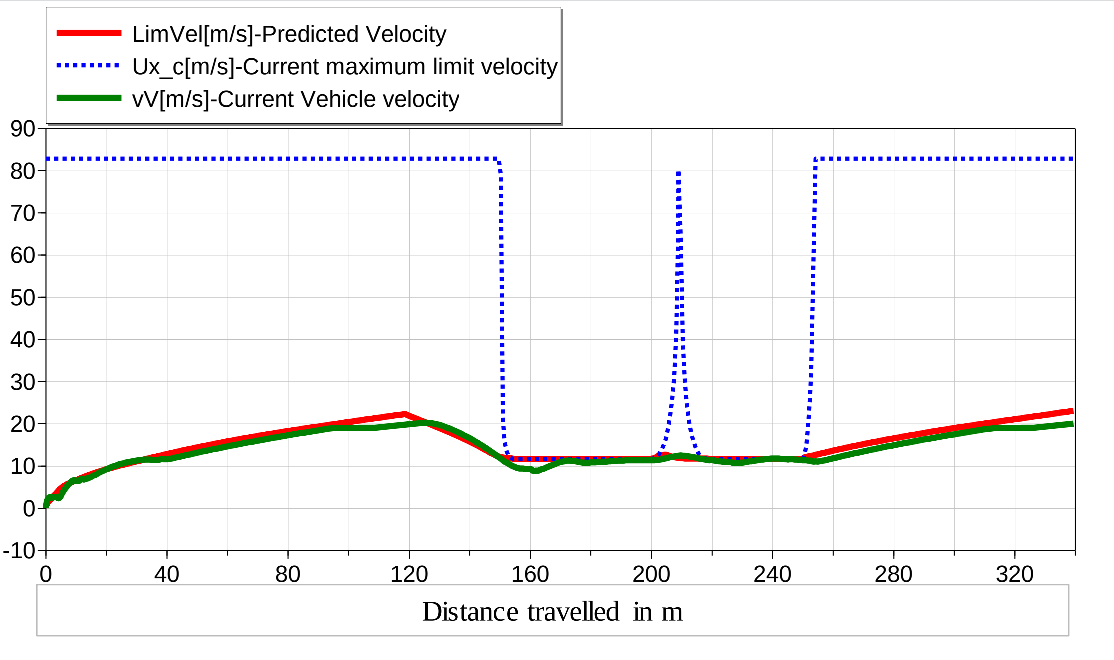

Figure 35: Velocity tracked by the CompactLEKPacejka02 model on extended chicane

Figure 35 shows the output of the velocity planning block on this track is similar to the previous simulation done using the FSAE race prototype (Figure 15) with only difference being that longitudinal and lateral acceleration values were different. The limits of handling were determined iteratively for this platform and they are as follows:

- Longitudinal Acceleration: 0.25 g
- Lateral Acceleration limit: 0.6 g
- Longitudinal Braking limit: 0.6 g.

It can be seen that the longitudinal acceleration of the actual vehicle is not a constant value and largely depends on what gear it is. For about 0-90 m the vehicle closely follows the output of the planning block but drops off a little when the top gear is engaged(at 100 m, *See* Figure 38). This is one more disadvantage of the velocity planning block, which assumes a constant acceleration capability throughout the range of gears. This leads to a minor overshoot of the braking point and hence there is the vehicle velocity dips below the target. But for the rest of track, the target velocity is tracked reasonably well. (The track runs out at 300 m, hence the output seen after that must be disregarded).

- **Tyre-Friction utilized**

The front axle is driven. The engine used doesn't seem capable of pushing the car to use up all of the friction on the straight line. Figure 36 shows that only 40 % of the friction is used during acceleration. During the LH turn, the front left tyre becomes the inside wheel, unloads due to lateral load transfer and undergoes longitudinal and lateral slip, while on the RH curve the front right tyre demonstrates this behaviour. These limit the achievable limit lateral acceleration to 0.6 g. Overall the front axle saturates during the turns and hence the vehicle understeers.

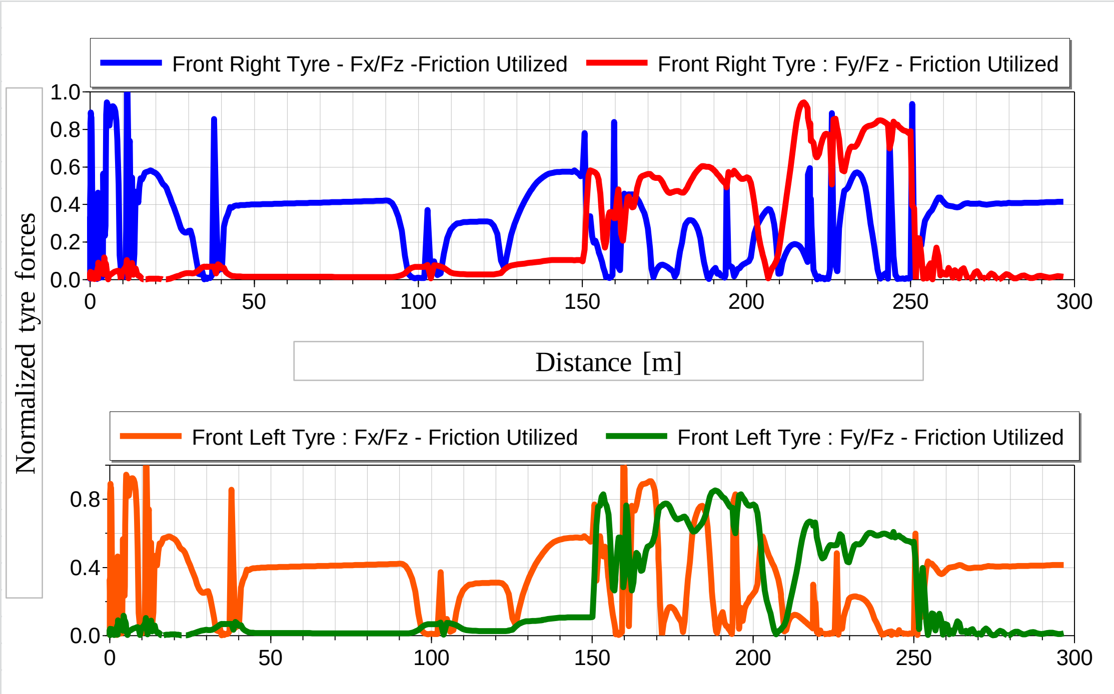

Figure 36: Tyre-Friction utilized: Front axle

The friction levels on the rear axle become nearly zero at full braking. Figure 37 shows that due to longitudinal load transfer nearly the entire rear axle is unloaded at 140 m at maximum braking. On the turns, an average of 70 % of the friction is utilized.

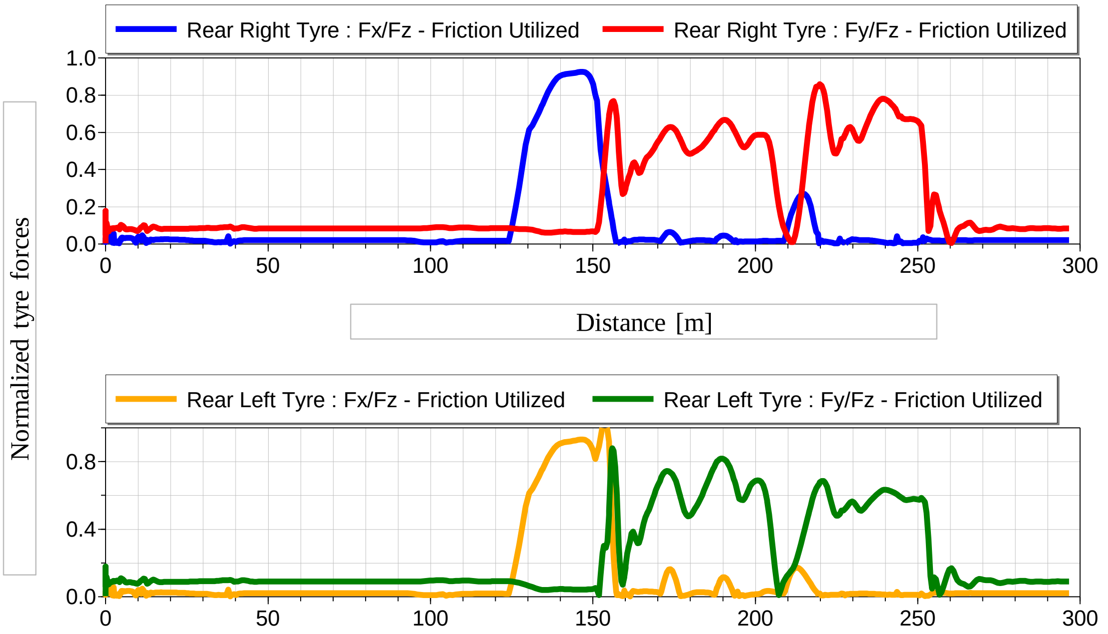

Figure 37: Tyre-Friction utilized: Rear axle

- **Longitudinal control of the vehicle**

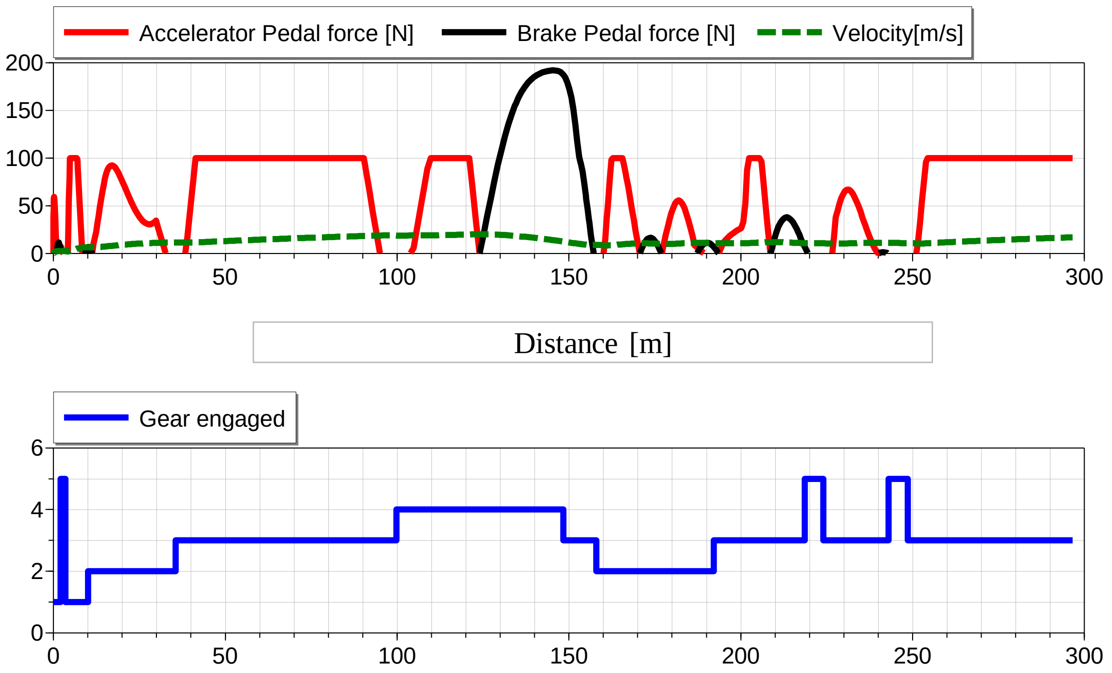

Figure 38: Control actions executed by the driving (throttle, gear, brake) robot over the velocity range

The gear shifting robot unnecessarily shifts into higher gear when the vehicle starts from standstill. Then short shifts to 2nd and then 3rd, only after which the vehicle is driven at full throttle. The maximum braking force was 200N and vehicle is decelerated at full braking. The gear correctly shifts down to 2nd gear during the first turn and then shifts up to 3rd during the second RH curve (from around 200 m). The throttle and brakes are operated simultaneously during the curves to maintain the vehicle speed close to the target. Unnecessary gear shifting is again on corner exit.

- **G-G plot**

  The target values of longitudinal acceleration of 0.25 g and deceleration of 0.6 g were achieved on the straights. During the curves the lateral acceleration target of 0.6 g was also achieved. It is quite evident that the vehicle is driven close to the edge of the friction ellipse.

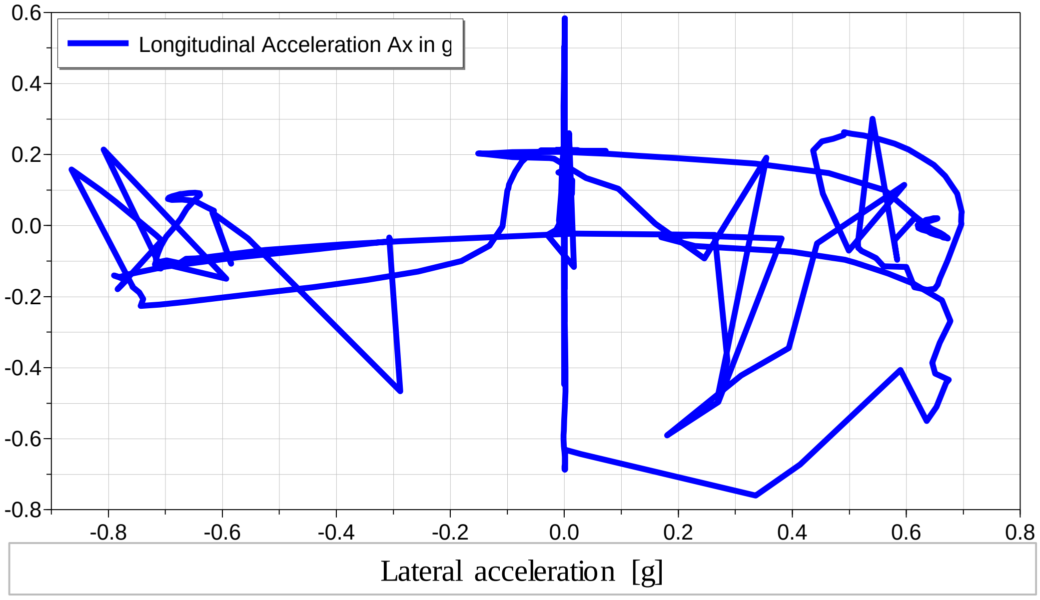

Figure 39: G-G plot for the extended chicane

4.4.2 Circle – constant radius

- Velocity tracking:

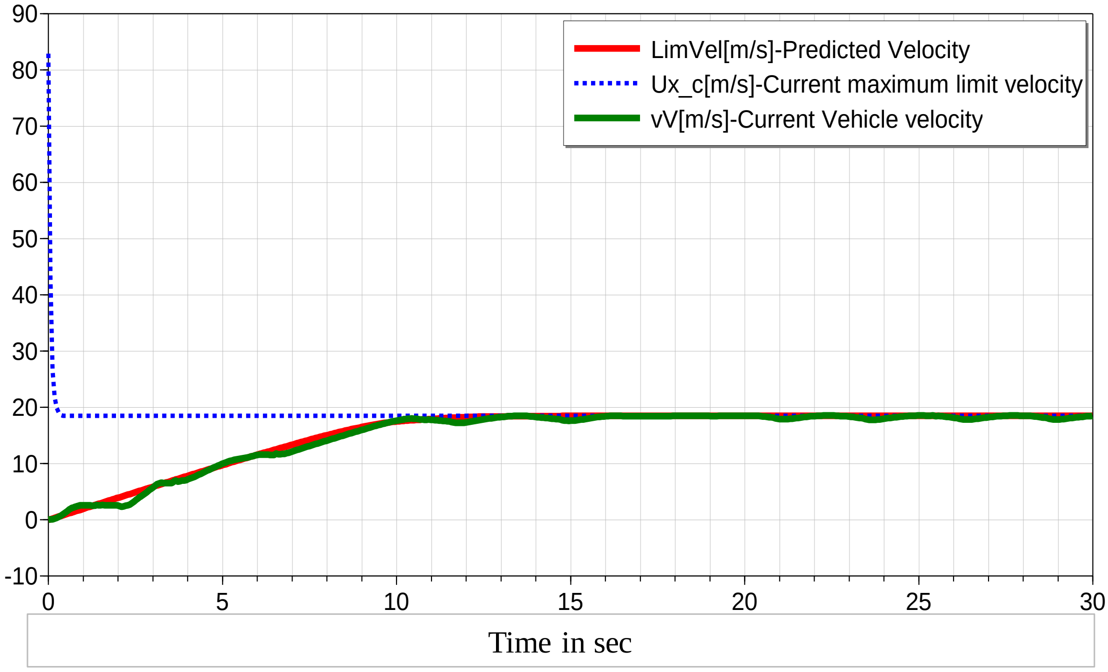

Figure 40: Velocity tracked by the CompactLEKPacejka02 model on the Oval

The velocity output is tracked really well by the vehicle model. Two laps were done on the circular track of constant radius. Initially a slight dip is seen when the vehicle speed reduces slightly below the target output by the velocity planning block. The set point velocity is reached with a user specified acceleration of 0.25 g.

- **Tyre-Friction utilized**

On the RH turn, the front right tyre is the inside tyre. On the front driven axle, lateral and longitudinal load transfer reduces the load on the inside tyre and doesn’t grip anymore on the curve. The inside tyre, under combined longitudinal and lateral slip is utilized to about an average of 90 % (combined longitudinal and lateral)

The rear non-driven axle just undergoes mostly lateral slip. Again the inside wheel (right tyre) utilizes less friction compared to the outside tyre.

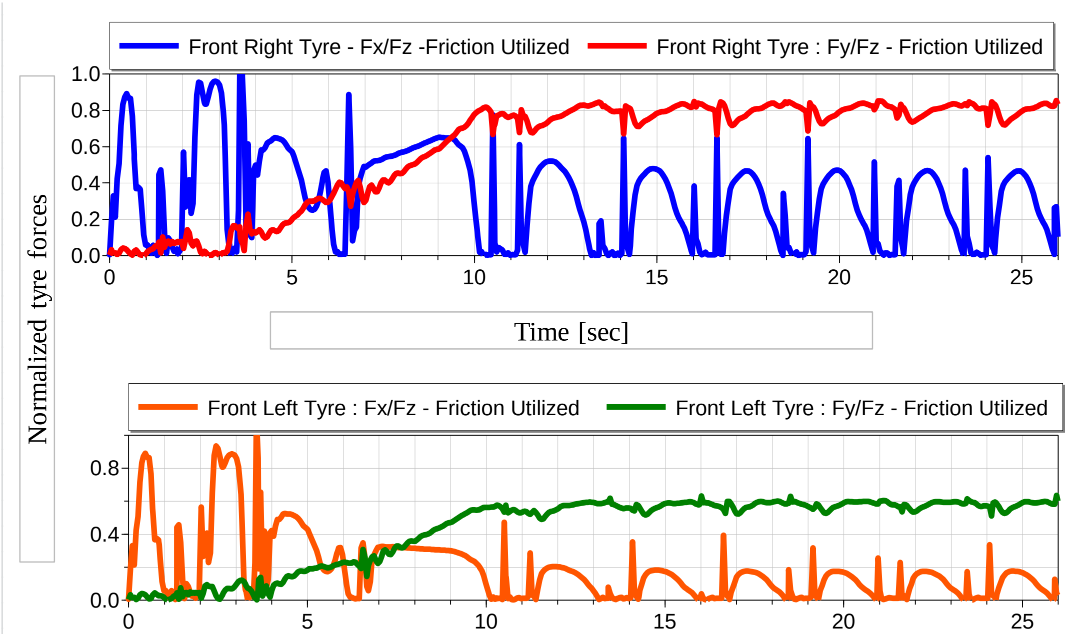

Figure 41: Tyre-Friction utilized: Front Axle

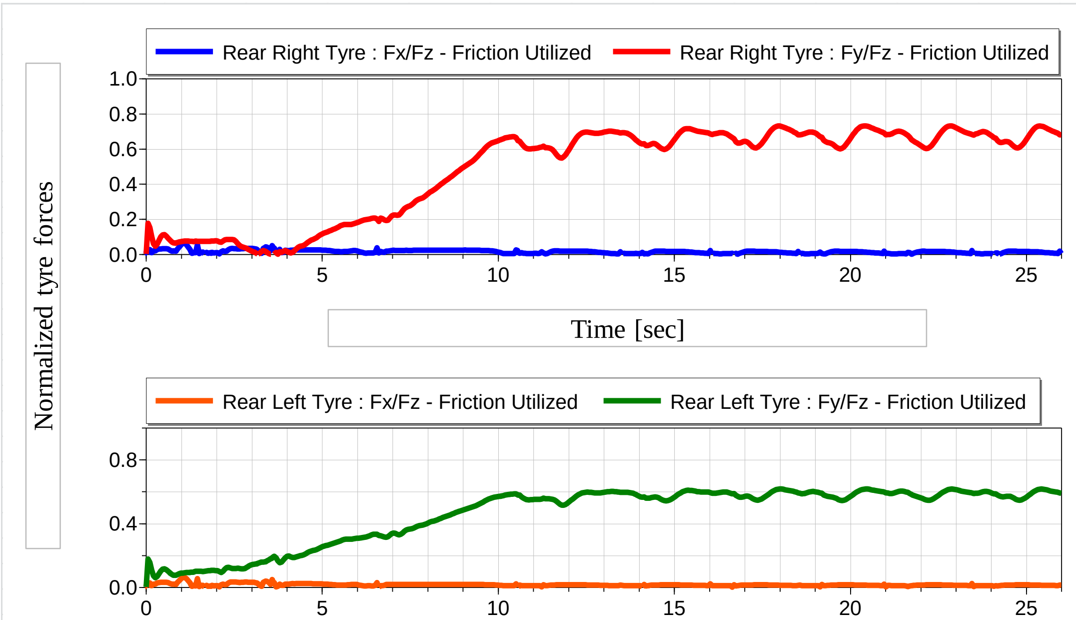

Figure 42: Tyre friction utilized: Rear axle

- **Longitudinal control of the vehicle**:

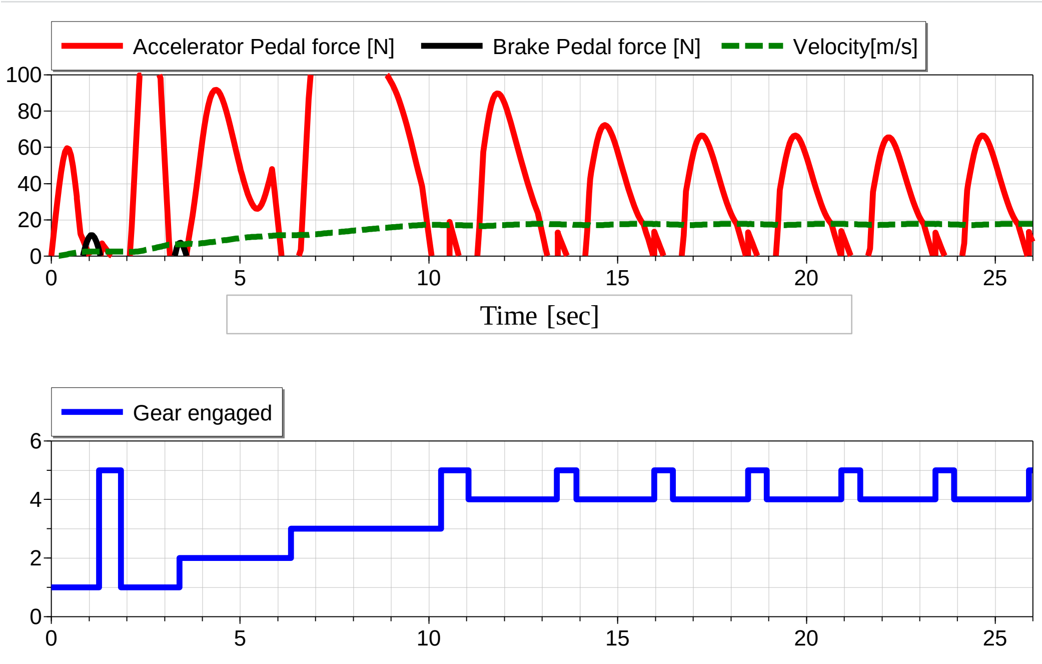

Figure 43: Control actions executed by the driving (throttle, gear, brake) robot over the velocity range

The gear robot again shifts unnecessarily during initial acceleration which is not ideal at all. Then it sequentially shifts up, applying full throttle to reach the target velocity. Once the target has been achieved, periodic throttle inputs maintain the vehicle speed with the target value. Brakes were never applied as the target look-ahead velocity is never exceeded at any point. The constant gear shifts seen in Figure 44 (after 10 sec) are undesirable and cause deceleration every time it shifts down, and an acceleration when the throttle is applied soon after. This can be seen in the G-G plot.

- **G-G plot**

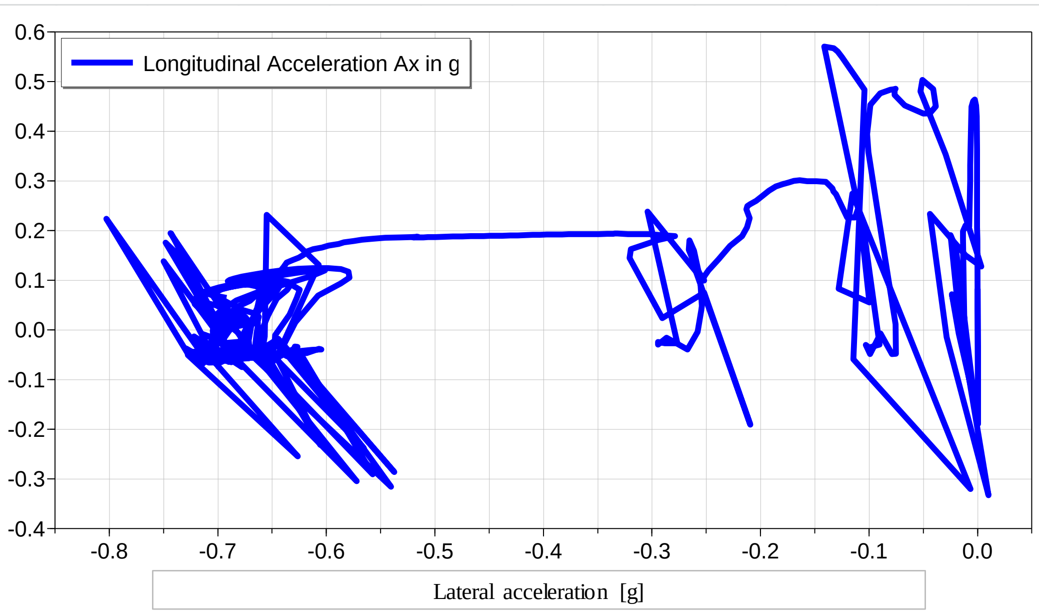

Figure 44: G-G plot for the Oval

The target lateral acceleration of 0.6 g was achieved but the constant gear shifting and the throttle inputs to maintain the target vehicle speed cause acceleration (around 0.2 g) and deceleration of -0.3 g.

4.4.3 Hi Speed J-turn:

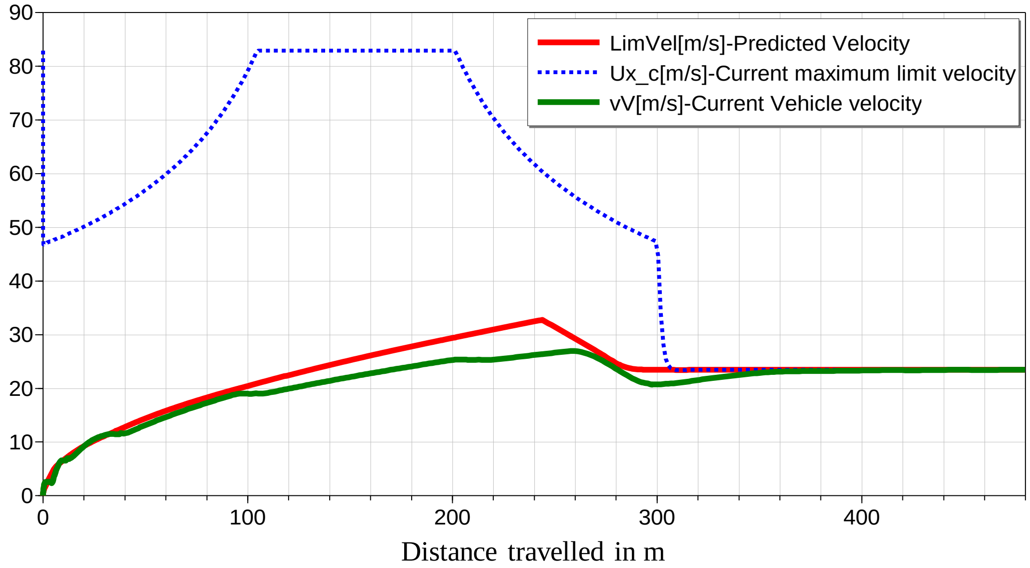

Figure 45: Velocity tracking on high speed J turn

This is the first time we see the output of the velocity planning block not being tracked well by the vehicle. The longitudinal acceleration constantly keeps falling as the vehicle accelerates to match the target speed. That eventually occurs very late, at least 20 m late. The brakes applied result in the vehicle dropping significantly below the target speed. The vehicle is then accelerated to reach the set point speed.

- **Tyre-Friction utilized**

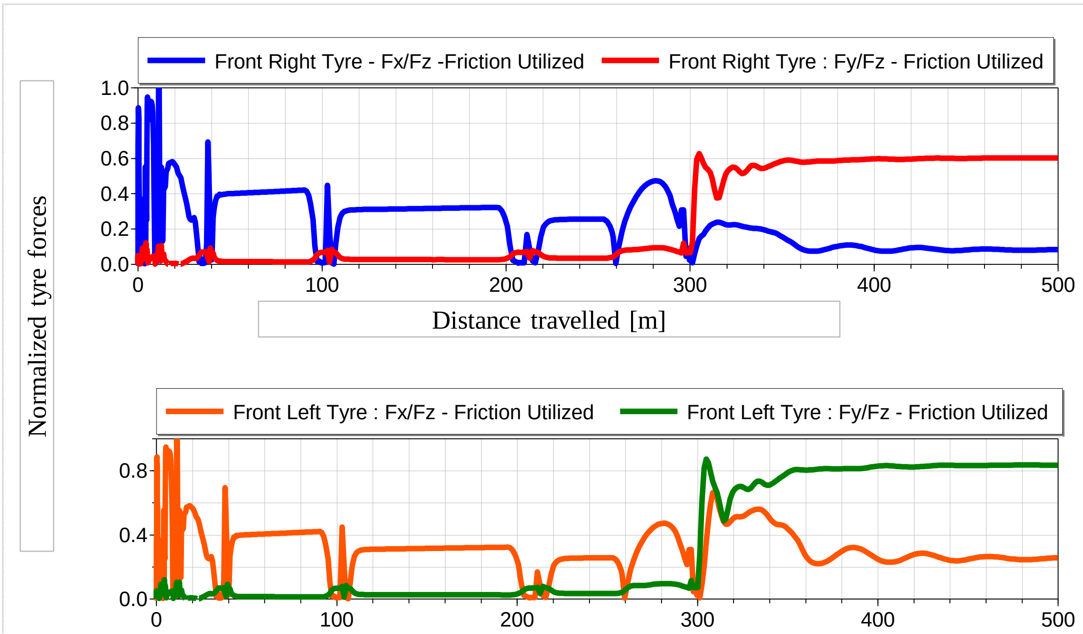

Figure 46: Tyre - Friction utilized: Front axle

Both axles are not entirely utilized to the limit. Only during the turn-in manoeuvre at 300 m do we see the inside (front left) tyre of the front driven axle under combined longitudinal and lateral slip. It is seen that both on the front and rear axles that the friction levels on the inside tyres are utilized around 80 % during the large LH turn. The outside tyres are use up to 60 % of the friction.

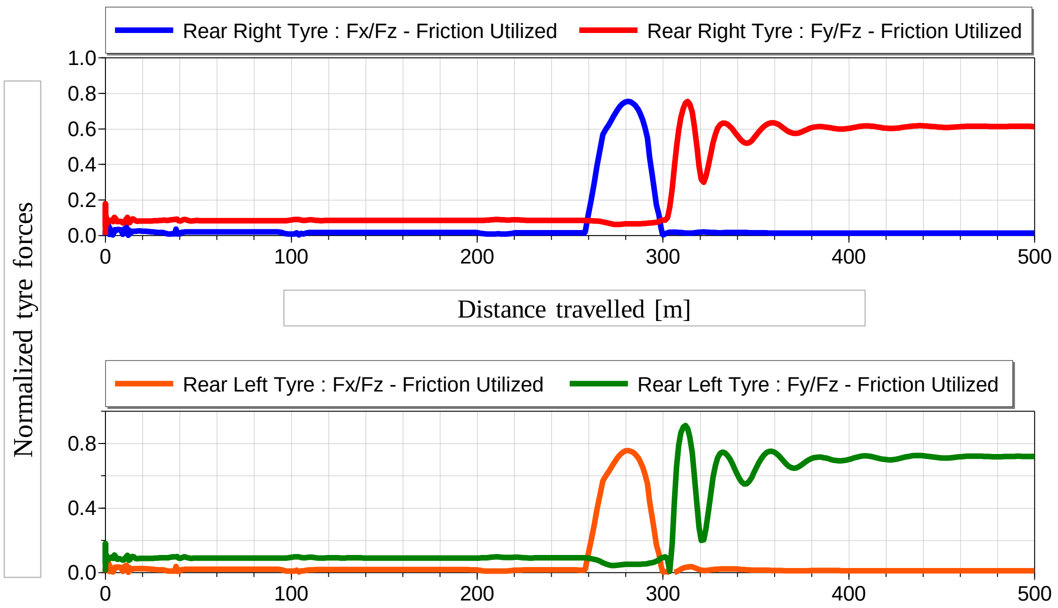

Figure 47: Tyre - Friction utilized: Rear axle

- **Longitudinal control of the vehicle**

The gear shifting robot again short shifts into top gear when car starts from standstill and then repeatedly short shifts to 3rd gear. This happens for about 40 m only after which full throttle is applied and the velocity increase with an acceleration of 0.25 g for about 100 m. (See slope of the plot line of vehicle speed in Figure 45). After this point, the 4th gear is engaged, even though at vehicle is at full throttle, the acceleration falls off target between 100 m and 260 m. Full braking force was 200 N, but due late braking, the deceleration required to reach the target speed was achieved with 75 % of the braking force. The target velocity on the curve is tracked very well.

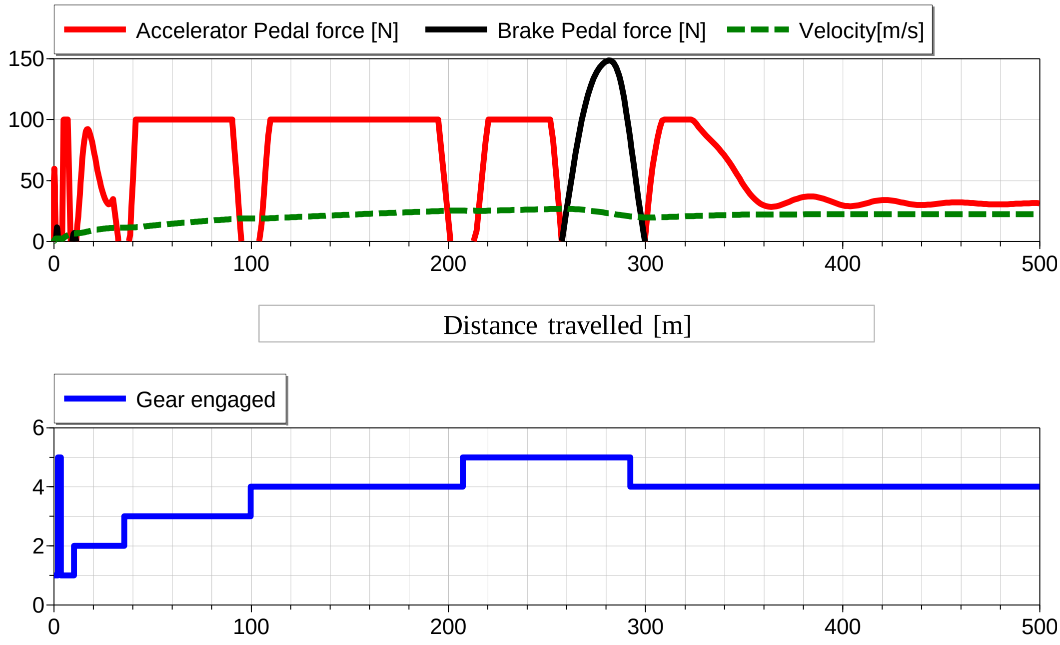

Figure 48: Control actions executed by the driving (throttle, gear, brake) robot over the velocity range

- **G-G plot**

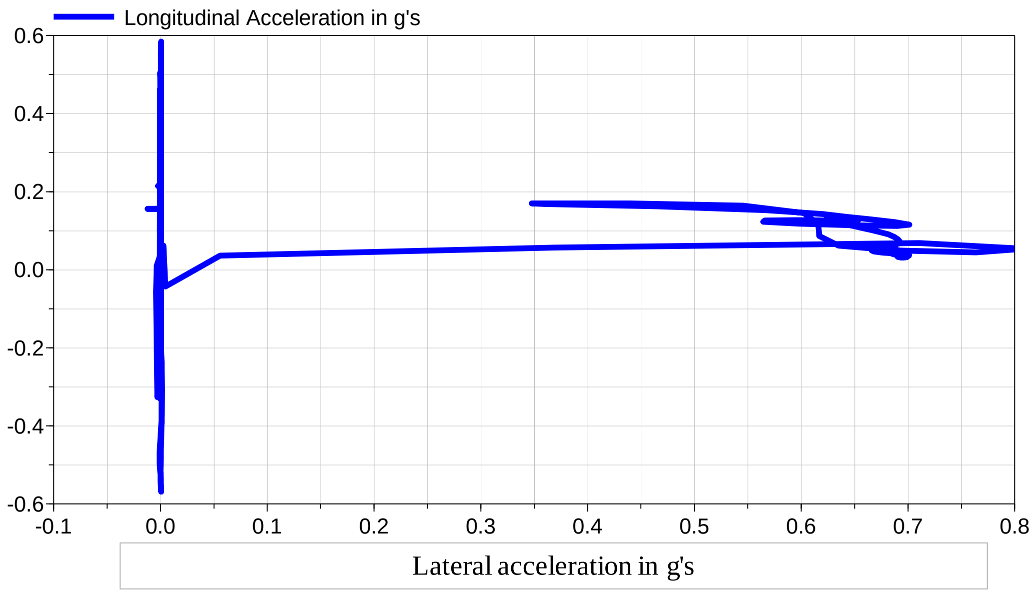

Figure 49: G-G plot on the high speed J turn

During the initially acceleration of the vehicle, a reading of 0.6 g in acceleration is registered but this is only an initial jerk. Although a deceleration of 0.6 g was achieved as specified it was quite unnecessary since the target velocity from which the vehicle had to brake with maximum capacity was never reached. On the LH turn, the target lateral acceleration was achieved.

4.4.4 Clothoid hairpin:

The numerical stability of the velocity planning block is tested, this time using the passenger car as the vehicle model on the Clothoid.

- **Velocity tracking**

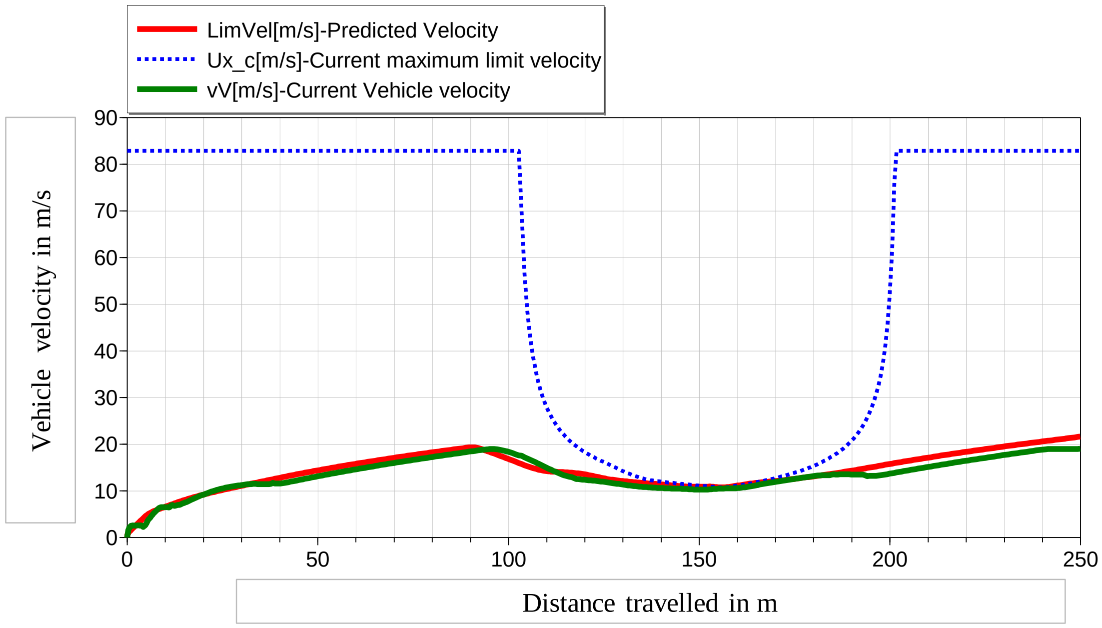

Figure 50: Velocity tracking on the Clothoid-Hairpin Curve

The velocity profile output is tracked down effectively by the vehicle. There is just a slight dip below the target at around 190 m, marking the corner exit point, due to the abrupt gear change.

- **Tyre-Friction utilized**

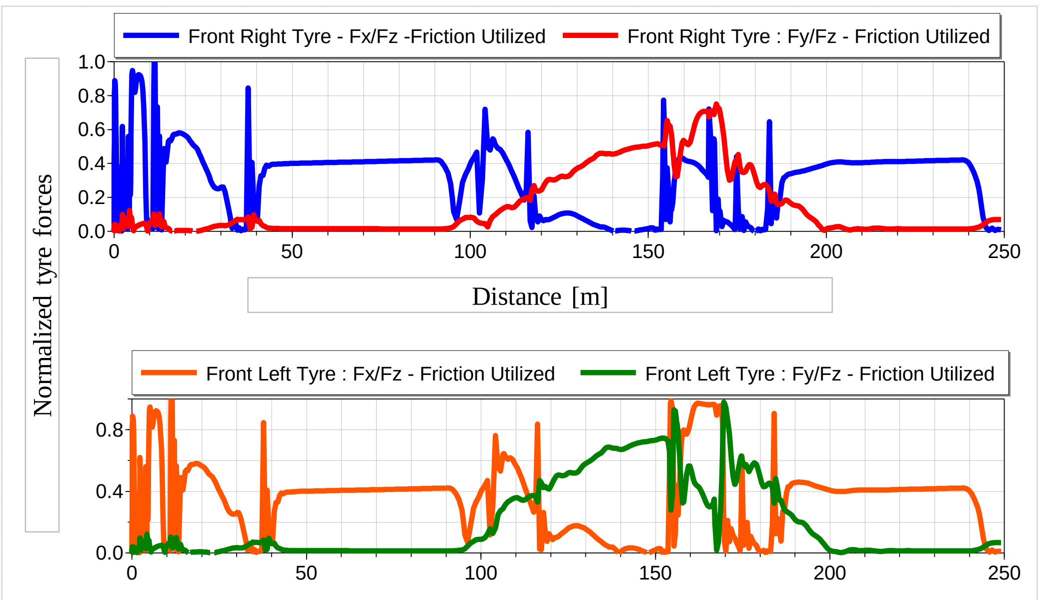

Figure 51: Tyre-Friction utilized: Front axle

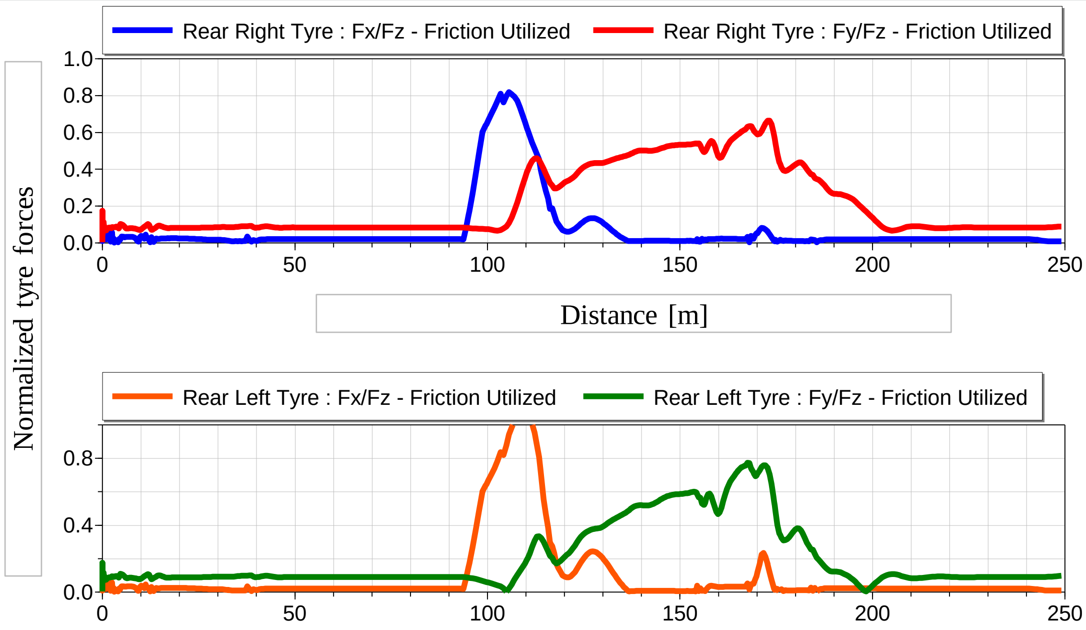

Figure 52: Tyre-Friction utilized: Rear axle

The front driven axle initially slips during start-up. Braking occurs at 105 m, during which the rear axle gets unloaded due to longitudinal load transfer and the front axle takes up most of the braking effort utilizing about 60 % of the friction. The tyre forces are gradually built up all the way till mid corner (at 150 m). The front left tyre on the driven axle is completely utilized under combined lateral and longitudinal slip. The front axle overall becomes saturated and limit understeer behaviour is seen. The rear axle however doesn't really saturate and uses about 60 % of friction on an average largely due to lateral slip.

- **Longitudinal control of the vehicle**

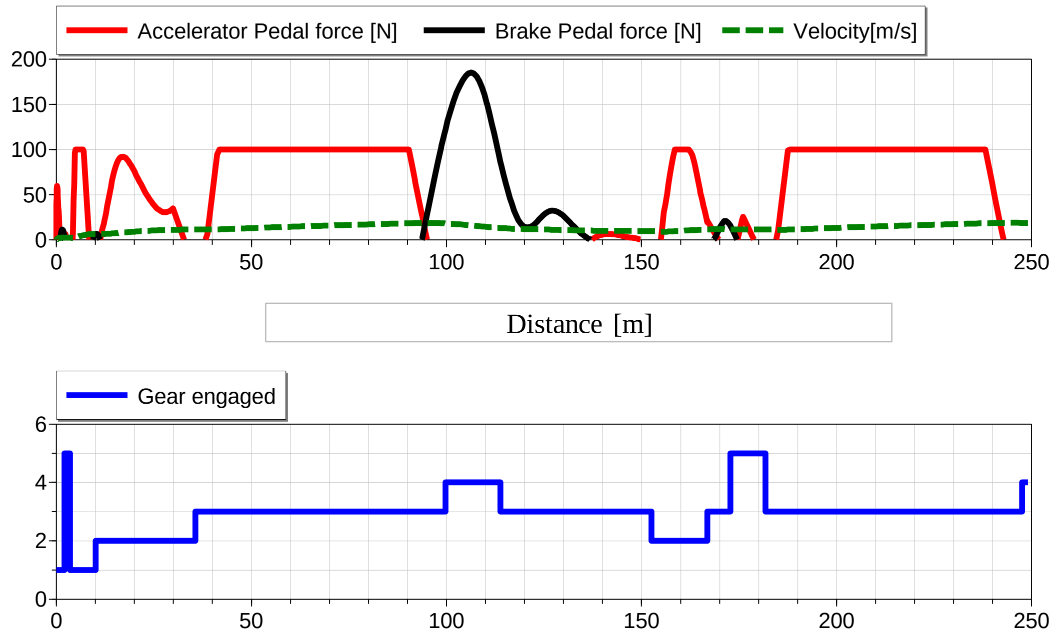

Figure 53: Control actions executed by the driving (throttle, gear, brake) robot over the velocity range

Similar to previous cases, it seems it takes about 40 m for the gear shifting robot to short shifting. Only after it engages 3rd gear, the vehicle is driven at full throttle. Now the vehicle does not short shift into 4th gear. Hence the acceleration of the vehicle during the straight line is as per the user input of 0.25 g. Hard braking ensures that the vehicle decelerates down to the target velocity. After mid-corner (150 m), when the vehicle needs to accelerate as per the input of the velocity planning block, the gear shifting robot unnecessarily short shifts into top gear, then immediately shifts down back to 3rd gear , only after which full throttle is engaged. This causes the slight dip seen at 190 m in Figure 50.

- **G-G plot**

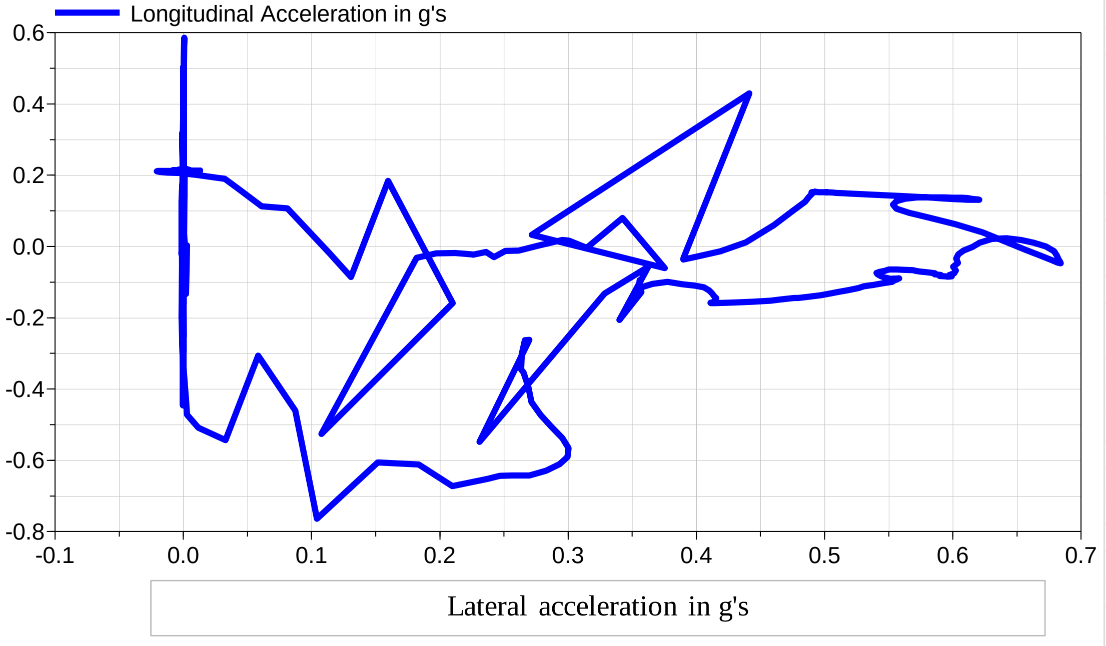

Figure 54: G-G plot on the hairpin curve

The initial jerk from start-up shows up as a reading of longitudinal acceleration of 0.6 g in Figure 54. Apart from this the targets of longitudinal and lateral acceleration/deceleration were achieved. The highest value of lateral acceleration was achieved at mid-corner.

4.5 Multi-point velocity planner:

In order to avoid the short comings of the single-point velocity planner, a multi-point velocity planning strategy was implemented. A total of 10 preview points were used. The distances of these ten points in front of the car was manually specified. This was tested only on the high-speed j-turn using the FSAE race prototype vehicle model.

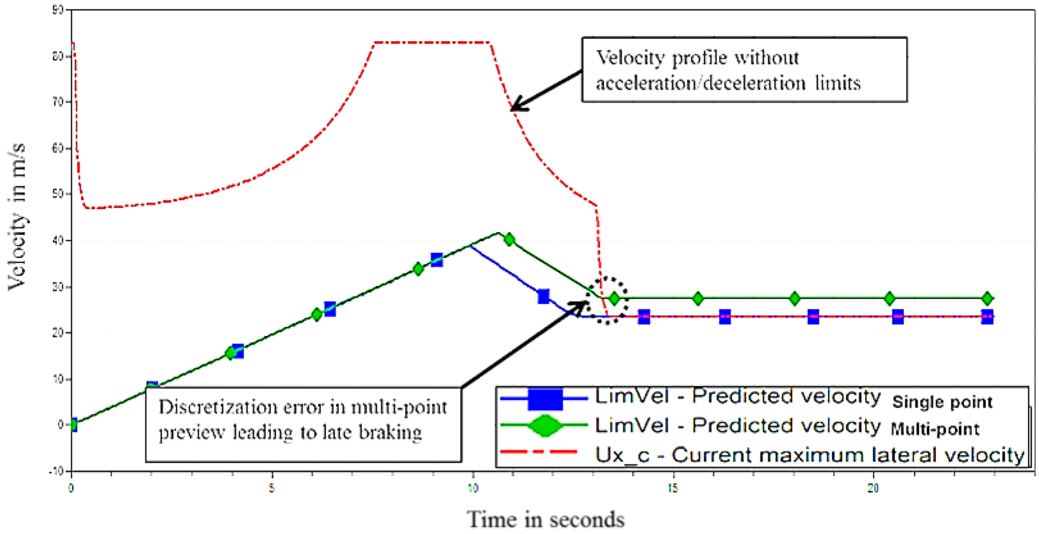

Figure 55: Result comparison between multi-point and single-point preview

The difference in the velocity planning can be seen from Figure 55. While the single-point preview brakes a bit early and stays on the conservative side, the multi-point preview brakes too late. This is due to the discretization error due to the limited number of preview points. The condition $v_{limit,n}^2 - v_{max}^2 < 2a_{x,n}s_n$ fails at a certain distance s_n at which the braking is not sufficient to reduce the current vehicle velocity to the limit velocity of the curve. *See* Figure 8.

The resolution of the preview points has to be increased and also tuned for every given track to achieve perfect braking just in time. Due to time limitation, this wasn't successfully implemented but can be looked at as a strategy in the future to make the driver model more robust and less conservative in braking.

5 Discussion

The goal of the thesis was to implement a velocity planning function within the current driver model setup without prior information of the track. The only source of information about the track available to the driver model comes from the preview information. Hence the preview distance is the most important function of the velocity planner.

In the single-point preview strategy, the preview distance was assumed to be the distance travelled by the vehicle when braking from the current velocity. This works well on long straights leading into a corner. In all the tracks tested, the preview point never failed to miss a road curvature and always initiated braking. How quickly this curvature is detected determines the timing of the initiation of the braking. The fact that the preview distance is calculated for the worst case scenario (distance required to come to standstill) is in itself conservative because the vehicle is required to slow down to the limit curvature velocity and does not need to come to a standstill. When this was tried, it was found that the preview signal was very hard to control. The preview point goes back and forth, as the vehicle velocity approaches the preview velocity. Therefore the current strategy implemented offers a robust solution. It is seen to be conservative only during the high-speed j-turn where it initiates braking earlier than it really needs to. *See* Figure 25.

Another factor that is difficult to estimate is the vehicle's braking capability. This is governed by the states the tyre are in, the longitudinal and the lateral slip they are undergoing. The maximum braking capability will be on a straight, where the lateral slip of a tyre is nearly zero while on a curve, with significant lateral slip of the tyre, especially if the vehicle is on or close the limit velocity, the braking capability is very much reduced. Since it is hard to predict the tyre slip, it is assumed that the vehicle always has the full braking and on this basis, the preview distance is calculated. The Clothoid/hair-pin circuit tests the effectiveness of this strategy and from the results, it can be seen that this is quite successful. This is due to the fact that the preview distance is calculated, as stated earlier, based on the need to bring the vehicle to a standstill from the current speed while the actual requirement is to only slow down to the upcoming curvature velocity. *See* Figure 30.

The multi-point preview strategy tried to overcome these limitations. It is effectively a brute force technique, where the number of preview points determines accuracy of the simulation points. The current implementation needs a larger number of preview points to work properly. Dymola, being primarily a physical modelling tool, is not the most suited environment to implement a larger set of preview points. Due to limited time, the full potential of this strategy was not tested but can be certainly worth looking into if the main criterion for developing a driver model remains to be limited a priori track information.

Tuning the PID controller:

For both vehicles the tuning was done once and that worked on four tracks. Most of the values were kept unchanged but the most significant difference was caused by the brake gain. The major difference between the FSAE racer prototype and the passenger vehicle is the weight, FSAE racer weighing 200 kg while the latter weighed 1100 kg.

The brake gain was reduced to a value of 20 and the maximum brake pedal force was limited to 40N. It must be noted that the brake system used for the FSAE racer was the same as that for the passenger car and it was selected from the VDL. This amounts to saying that having extremely large brakes on a very small vehicle. This justifies limiting the maximum brake pedal for to 40N that decelerated vehicle according to the target deceleration value of 0.6 g. Any larger value of brake gain or pedal force would result in the vehicle slowing doing way too much. If the deceleration target value of 1 or 0.95 g, then the larger brake gains have to be used to meet the target. And if done so, all tyres saturated completely, the vehicle becomes unsteerable and unstable and eventually goes off-track as it enters the curve. Thus by analysing the high speed braking stability, the limit of the vehicle's deceleration capability was found. In case of the passenger vehicle, the brake gain was increased to a value of 50 while the maximum pedal force was limited to 200N that was sufficient to achieve the target of 0.6 g.

The rest of the gains were kept around default values. The acceleration capability was eventually arrived by looking at vehicle speed at full throttle on the straights. The lateral acceleration limit was determined by observing the handling behaviour and tyre saturation levels. A final value of 0.7 g was determined as the limit for lateral acceleration for the FSAE racer while the passenger car could achieve a maximum of 0.65 g. The final settings of the PID controller are as tabulated below.

Parameter	Formula SAE prototype	CompactLEKPacejka02
K_brk - Brake gain	20	50
K_acc - Accelerator gain	0.9	1
K - Proportional gain	0.8	1
Ti - Integral gain	2	2
Td - Preview time horizon sec	1.0	1.0
N- Derivative filter	1e-6	1e-6
brk_dz- Braking velocity error dead-zone	0.0	0.0
Tt - Tracking time constant sec	Ti/4	Ti/4
f_max - Maximum brake pedal force N	40	200

Table 5.1: Parameters of PID Longitudinal controller

6 Conclusion

The online strategies implemented here will never be as fast as the offline lap simulations mentioned in section 2.1.1 but it is a more convenient way evaluating the characteristics of a vehicle within the present framework of the VDL. To achieve an optimal solution, more a priori track information is required.

If there is no mechanism to have the complete knowledge of the track beforehand, it is very challenging to tune the preview. In spite of these challenges of was seen that the solutions implemented were satisfactory and provides a basis for the future development of a complete racing driver model.

In the simulations performed, the vehicle's stability under high-speed braking, its acceleration capability on a straight line and its lateral acceleration limit and its behaviour were clearly seen and a measure of the handling capability of the vehicle in terms of longitudinal and lateral acceleration limits were obtained as shown below:

Table 6.1: Limit of Handling

Acceleration in g's	Formula SAE prototype	CompactLEKPacejka02
Longitudinal Acceleration	0.4	0.2
Longitudinal Deceleration	0.6	0.6
Lateral Acceleration	0.7	0.65

It must be kept in mind that the boundaries outlined above are indicative of the values at which the vehicle is stable in all the tracks tested. For example, the absolute limit of longitudinal deceleration/braking might be more than 0.6 g but becomes impossible to manoeuvre at higher values, i.e., if the vehicle only had to come to a complete standstill on only a straight line , then the limit would have been higher. But what one is interested at what point the vehicle goes out of control, as a stability boundary.

With a similar argument, all other limits were found out for both vehicles. For e.g., the true lateral acceleration level achievable on a curve of a very large radius will be higher than on a curve of a very small radius. But the methods adopted in this thesis works well on the 4 tracks created which have a smooth curvature signal and experienced no numerical instability and provide an easy and convenient method to obtain a measure of the handling limits of a vehicle.

7 Future Work

Section 1.4 mentions the delimitations of the project and these aspects, among others, should be included in the development of the final "Racing driver" model.

The primary improvement needs to be made in terms of processing the track information. Expanding the single point strategy into the multi-point preview strategy, could be one method. If the information on the curvature and friction level is known beforehand, then driver model can be made more robust and reliable.

As explained in section 2.1.1, lateral planning affects the lap-time around a circuit to a great extent and would also allow manoeuvres like the double-lane change to be simulated. The added capability measuring 3-D curvatures and uphill and downhill roads will provide a substantial value for the driver model. Ultimately, efforts should be made in exploring methods to make the preview horizon optimal.

Also, it must be noted that the vehicle's longitudinal acceleration capability differs with every gear; hence instead of the user having to input this value, a simple vehicle model might be implemented that calculates the longitudinal acceleration when the gear is changed. But this of course implies that gear selection and gear shifting be optimized. It was seen in the case of simulations performed using the compact car model, especially in section 4.4.3, that the abrupt gear changes had a profound effect on the vehicle speed.

The inclusion of aero-dynamics package would be the last step in producing a complete racing driver model. A function, entered by the user, which correlates the increase in vehicle speed with the amount of downforce, may be used and a scaling factor for the accelerations may be incorporated within the current framework. But the additional grip generated due to aerodynamic downforce and resistance encountered due to aerodynamic drag effects needs to be numerically modelled, in order to accurately estimate vehicle speed profile around a given track. Only then would the velocity profile generate push the vehicle to the edge of its handling capability

8 References

[1] Kritayakirana.K, Gerdes.J.C. (2010), - Autonomous Cornering at the Limits: Maximizing a “g-g” Diagram by Using Feed-forward Trail-Braking and Throttle-on-Exit, 6th IFAC Symposium July 2010

[2] Braghin. F, Cheli. F, Melzi. F, Sabbioni. F. (2007), Race driver model, Politecnico di Milano, Department of Mechanics

[3] Milliken.W.F. and Milliken.D.L. (1995), Race Car Vehicle Dynamics, SAE International No. 287-359.

[4] Sharp.R.S, Casanova, D., Symonds, P. (2000), A Mathematical Model for Driver Steering Control, with Design, Tuning and Performance Results, Vehicle System Dynamics, 33 pp. 289–326

[5] Xiong.Y (2010), Racing line optimization, Computation for design and Optimisation, Massachusetts Institute of Technology.

[6] Gustafsson.T, Sjöberg.J, Åslund.J (2008), Computing the Ideal Racing Line Using Optimal Control, ISY, Linköpings University

[7] Vehicle Dynamics Library, version 1.5, Users Guide; Modelon AB

[8] Thomson.R, Dr.Jacobson, Bengt. (2007) Lecture Notes for Vehicle Dynamics, Department of Applied Mechanics, Chalmers University of technology

[9] Ahmed U, Solis.J, (2012), Mossberg.M Steering Controller design in Dymola VDL, Karlstad University, Sweden,

[10] Subbanna.A.K, Bruzelius.F, Drenth.E, Torstensson.I, Sundström.P (2012), Velocity Planning for a Racing Driver Model, Proceedings of the 11th International Symposium on Advanced Vehicle control.